

RESEARCH ARTICLE

Arf activation at the Golgi is modulated by feed-forward stimulation of the exchange factor GBF1

Douglas Quilty¹, Fraser Gray¹, Nathan Summerfeldt¹, Dan Cassel² and Paul Melançon^{1,*}

ABSTRACT

ADP-ribosylation factors (Arfs) play central roles in the regulation of vesicular trafficking through the Golgi. Arfs are activated at the Golgi membrane by guanine-nucleotide-exchange factors (GEFs) that are recruited from cytosol. Here, we describe a novel mechanism for the regulation of recruitment and activity of the ArfGEF Golgi-specific BFA resistance factor 1 (GBF1). Conditions that alter the cellular Arf-GDP:Arf-GTP ratio result in GBF1 recruitment. This recruitment of GBF1 occurs selectively on cis-Golgi membranes in direct response to increased Arf-GDP. GBF1 recruitment requires Arf-GDP myristoylation-dependent interactions suggesting regulation of a membrane-bound factor. Once recruited, GBF1 causes increased Arf-GTP production at the Golgi, consistent with a feed-forward self-limiting mechanism of Arf activation. This mechanism is proposed to maintain steady-state levels of Arf-GTP at the cis-Golgi during cycles of Arf-dependent trafficking events.

KEY WORDS: Golgi, Arf, GTPase, GBF1, Brefeldin A

INTRODUCTION

The Golgi functions as a central organizing organelle in the secretory pathway (Farquhar and Palade, 1998; Emr et al., 2009). The central Golgi stack (consisting of cis-, medial- and trans-cisternae) processes and facilitates the targeting of newly synthesized cargo proteins as they emerge from the ER-Golgi intermediate compartment (ERGIC) and traffic through the trans-Golgi network (TGN). The exact mechanism through which individual compartments are created and maintained remains unknown, but it is generally assumed that the recruitment of protein factors to a specific compartment is required to establish and define each compartment (Lippincott-Schwartz, 2011).

Members of the Arf family of small GTPases play central roles in vesicular trafficking at the Golgi. Primate cells express five Arf proteins (Arf1, 3, 4, 5 and 6) that are classified into three classes (class I: Arf1 and Arf3; class II, Arf4 and Arf5; and class III, Arf6). Class I and II Arfs are found differentially distributed through the Golgi (Dejgaard et al., 2007; Chun et al., 2008; Manolea et al., 2010). Arf proteins exert their regulatory effect through cycles of GTP binding and hydrolysis, induced by Arf guanine-nucleotide-exchange factors (GEFs) and Arf GTPase-activating

proteins (GAPs). Activation of Arf proteins occurs at the membrane and requires simultaneous membrane association of both substrate and the activating GEF (Cherfils and Melançon, 2005). The initial association of Arfs with membranes depends on its N-terminal myristoyl moiety (Haun et al., 1993; Randazzo and Kahn, 1995; Franco et al., 1996; Tsai et al., 1996), whereas stable association is triggered upon GTP-induced locking of the exposed N-terminal amphipathic motif (Pasqualato et al., 2002). Recent work has suggested that initial Arf association with membranes further depends on Arf receptors that are present in the Golgi membrane (Gommel et al., 2001; Honda et al., 2005).

It is well established that the Golgi is sensitive to the drug brefeldin A (BFA) (Fujiwara et al., 1988; Doms et al., 1989; Lippincott-Schwartz et al., 1989). This drug acts as a non-competitive inhibitor of a sub-family of large ArfGEFs that includes GBF1 (Golgi-specific Brefeldin A-resistance factor 1) and BIGs (BFA-inhibited GEFs) (Casanova, 2007). Whereas GBF1 localizes to and functions at the early Golgi, BIGs function at the TGN (Kawamoto et al., 2002; Zhao et al., 2002; Zhao et al., 2006; Manolea et al., 2008). Thus, GBF1 appears to be the primary, if not only, GEF responsible for activation of class I and class II Arfs at the ERGIC and cis-Golgi membranes.

The fact that Arf activation must occur at the membrane surface emphasizes the importance of studying the recruitment of GBF1 to Golgi membranes. Much of the information available on the function of ArfGEFs such as GBF1 is derived from use of the inhibitor BFA (Melançon et al., 2003; Casanova, 2007). Several *in vitro* studies have established that the catalytic sec7 domain of sensitive GEFs forms a stable, non-productive complex with BFA and substrate Arf-GDP (Sata et al., 1998; Mansour et al., 1999; Peyroche et al., 1999; Robineau et al., 2000; Mossessova et al., 2003; Renault et al., 2003). Furthermore, several groups have reported that BFA treatment causes accumulation of GBF1 on Golgi membranes in live cells (Niu et al., 2005; Szul et al., 2005; Zhao et al., 2006). These results led to the hypothesis that release of GBF1 from membranes is linked to the completion of the nucleotide exchange reaction, a process that is blocked in the presence of BFA (Niu et al., 2005; Szul et al., 2005).

The model described above predicts co-accumulation of GBF1 and Arf on Golgi membranes following BFA treatment. Our laboratory tested this prediction using live-cell imaging but failed to detect accumulation of the Arf at the Golgi (Chun et al., 2008). Rather, we observed rapid release of Arfs from Golgi membranes, concurrently with GBF1 accumulation. In the present study, we examined the recruitment of GBF1 on Golgi membranes using several independent approaches. Our findings indicate that GBF1 accumulation on membranes is sensitive to the Arf-GDP:Arf-GTP ratio, which can explain the BFA effect. We propose that the recruitment of GBF1 to Golgi membranes is part of a homeostatic

¹Department of Cell Biology, University of Alberta, Edmonton, AB T6G 2H7, Canada. ²Department of Biology, Technion-Israel Institute of Technology, Haifa 32000, Israel.

*Author for correspondence (Paul.Melancon@UAlberta.ca)

regulatory mechanism that functions to maintain proper Arf-GTP levels on cis-Golgi membranes.

RESULTS

GBF1 accumulates on Golgi membranes in response to an increase in the ratio of Arf-GDP to Arf-GTP

Previous studies have revealed that treatment with BFA caused a dramatic accumulation of GBF1 on Golgi membranes (Niu et al., 2005; Szul et al., 2005; Zhao et al., 2006). As mentioned above, further work from our laboratory indicated that GBF1 accumulation is not accompanied by recruitment of Arfs (Chun et al., 2008). We further observed that treatment of NRK cells with Exo1, a drug that reduces Arf-GTP levels but does not target the GEF, also caused recruitment of exogenous GBF1 to Golgi and ERGIC membranes. To confirm and extend these results, we tested the effect of Exo1 treatment on endogenous GBF1 localization in HeLa cells. We first confirmed that in live HeLa cells expressing mCherry-GBF1 and treated with 200 μ M Exo1 for 1 minute, GBF1 is clearly recruited to Golgi and peripheral puncta (Fig. 1A). No change in mCherry-GBF1 localization and recruitment was observed in control cells treated with DMSO for 1 minute. To ascertain that Exo1-dependent accumulation did not depend on overexpression of tagged GBF1, we tested its effect on the endogenous protein. Treatment of HeLa cells with 200 μ M

Exo1 for 1 minute caused Golgi recruitment of endogenous GBF1 (Fig. 1B) similar to that observed for exogenous mCherry-GBF1 (Fig. 1A). Quantification of endogenous GBF1 recruitment, shown as a ratio of mean Golgi intensity to mean cytosol intensity, revealed a 2.5-fold increase in Golgi-localized GBF1 following a 1-minute Exo1 treatment (Fig. 1C).

To obtain independent evidence that the ratio of Arf-GDP to Arf-GTP influences GBF1 recruitment, we examined the impact of ArfGAP1 overexpression on GBF1 distribution. Previous studies have established that ArfGAP1 localizes to the Golgi where it promotes GTP hydrolysis on Arfs (Cukierman et al., 1995; Szafer et al., 2001; Shiba et al., 2011). Further characterization of the N-terminal GAP domain identified a crucial ‘arginine finger’ residue that participates in catalysis (Szafer et al., 2000; Ismail et al., 2010), and mutation of this arginine residue (residue 50 in human ArfGAP1) abrogated GAP activity *in vivo* (Shiba et al., 2011). To examine the potential role that the ratio of Arf-GDP to Arf-GTP played in GBF1 recruitment, we examined the distribution of endogenous GBF1 in HeLa cells transiently expressing low levels of EGFP-tagged wild-type (WT) or the catalytically dead R50Q point GAP1. This experiment revealed an increase in Golgi-localized GBF1 in cells expressing WT EGFP-GAP1. Interestingly, expression of inactive EGFP-GAP1 R50Q resulted in a clear and significant

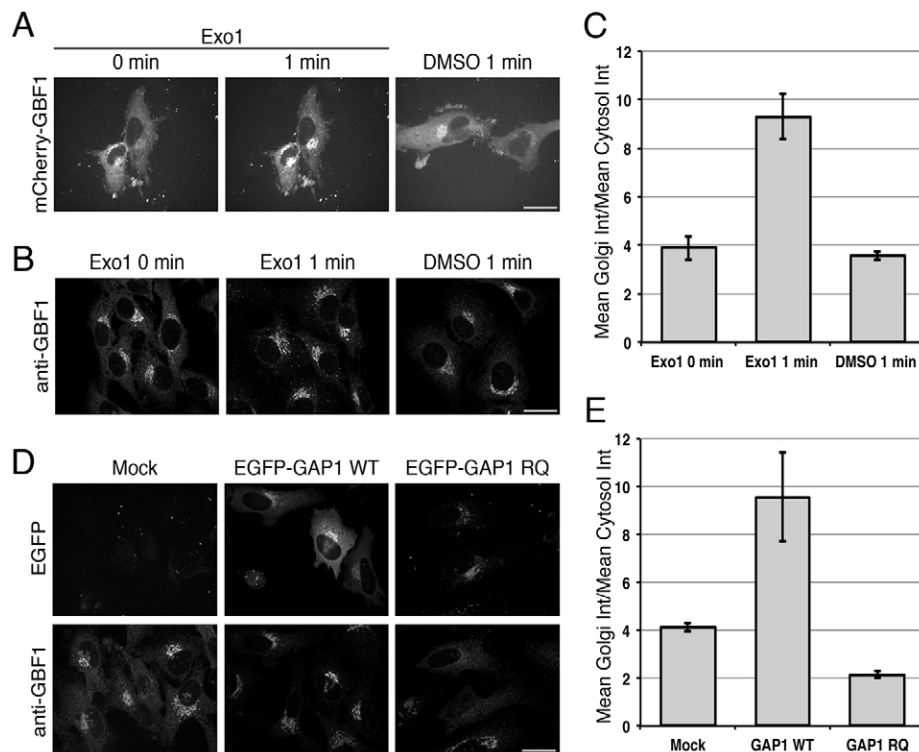


Fig. 1. Changes in the cellular Arf-GTP:Arf-GDP ratio cause the recruitment and accumulation of GBF1 on Golgi membranes. (A) HeLa cells expressing mCherry-GBF1 were treated with 200 μ M Exo1 or DMSO as a control and imaged by live cell spinning disc confocal microscopy as described in the Materials and Methods. Cells from a representative experiment ($n=6$) are displayed as focal projections of all z-slices. (B) HeLa cells were treated with 200 μ M Exo1 or DMSO as a control then stained with mouse anti-GBF1 monoclonal antibody and imaged by fixed cell spinning disc confocal microscopy. Cells from a representative experiment ($n=3$) are displayed as focal projections of all z-slices. (C) Quantification of GBF1 recruitment in cells treated with Exo1 or DMSO-only was performed by measuring the ratio of mean intensity (Int) of GBF1 staining at the Golgi to mean intensity of GBF1 staining in the cytosol. A minimum of eight cells similar to those shown in B were quantified in each of three separate experiments. (D) HeLa cells were mock transfected or transfected with plasmids encoding EGFP-GAP1 WT or EGFP-GAP1 RQ. Cells were then fixed and stained with mouse anti-GBF1 monoclonal antibody and imaged by spinning disc confocal microscopy. Cells from a representative experiment ($n=3$) are displayed as focal projections of all z-slices. (E) Quantification of GBF1 recruitment in images like those shown in D was performed as described for panel C. A minimum of eight cells were quantified in each of three separate experiments. Scale bars: 26 μ m.

decrease in membrane-associated GBF1 relative to mock-transfected control cells (Fig. 1D). Quantification of the ratio of Golgi-bound to free cytosolic GBF1 showed that expression of WT ArfGAP1 resulted in a 2.5-fold increase in ratio of Golgi-associated to free GBF1 relative to that in the mock-transfected control (Fig. 1E). In contrast, expression of ArfGAP1 R50Q caused a 50% reduction in this ratio. This unexpected observation suggests that expression of catalytically inactive ArfGAP decreases the Arf-GDP:Arf-GTP ratio. Altogether, our results suggest that GBF1 recruitment responds to re-establish steady state Arf-GTP level, and is sensitive to both increases and decreases of the cellular ratio of Arf-GDP to Arf-GTP.

Arf-GDP promotes accumulation of GBF1 on Golgi membranes

Sensing a change in the ratio of Arf-GDP to Arf-GTP can result from responding to either the GDP- or the GTP-bound form of Arf. The potential involvement of Arf-GDP could be readily tested utilizing a well-characterized the T31N point mutation that interferes with GTP binding and maintains Arf in an inactive state (Dascher and Balch, 1994). In order to perform this experiment, we first had to develop a method that would allow expression of dominant-inactive Arf1 T31N-EGFP while maintaining the integrity of the Golgi because expression of this dominant-inactive mutant causes a collapse of the Golgi and a block in protein traffic (Dascher and Balch, 1994; Donaldson et al., 2005). To achieve this, we first optimized transfection conditions to

achieve low levels of Arf expression. To prevent Golgi collapse, we coexpressed myc-tagged memrin, a Golgi SNARE that can recruit Arf1-GDP to the Golgi. Overexpression of either GBF1 (Claude et al., 1999) or memrin (Honda et al., 2005) had previously been shown to protect from BFA-induced Golgi collapse (Honda et al., 2005), probably as a result of sufficient Arf1-GTP production. We speculated that memrin overexpression would similarly prevent Arf1-T31N-induced Golgi collapse through enhanced production of Arf1-GTP by more efficiently recruiting Arf1-GDP to the site of activation. The distribution of GBF1 was therefore examined in HeLa cells coexpressing myc-memrin, and either the WT or T31N mutant forms of Arf1-EGFP. To assess relative Arf overexpression in our experiment, we performed quantitative western blot analysis as described in the Materials and Methods. We observed that relative band intensities of the exogenously expressed Arf-EGFP (about 45 kDa) and endogenous Arf (about 20 kDa) were similar (Fig. 2A). The anti-GFP antibody panels confirm that our Arf antibody detects the overexpressed protein. We determined that the fold overexpression of Arf1 WT-EGFP and Arf1 T31N-EGFP was 1.4-fold and 0.9-fold, respectively (Fig. 2B).

We next examined GBF1 distribution in cells expressing low levels of WT and mutant Arf1. Initial experiments focused on the distribution of mCherry-GBF1. As predicted by Honda et al. (Honda et al., 2005), the integrity of the Golgi was maintained in a significant fraction of cells coexpressing myc-memrin,

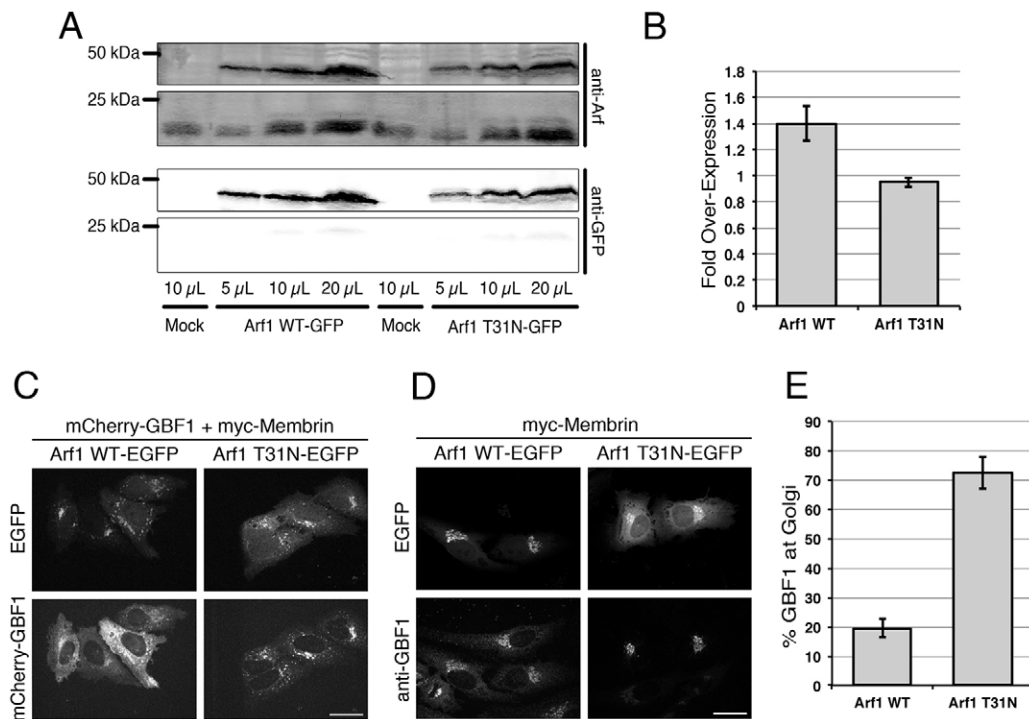


Fig. 2. Increases in Arf-GDP levels cause the recruitment and accumulation of GBF1 on Golgi membranes. (A) Western blot analysis of post-nuclear extracts prepared from HeLa cells transfected with plasmids encoding mCherry-GBF1, myc-memrin, and either WT or T31N forms of Arf1-EGFP. Different volumes of each sample were analyzed to ensure that the signal remained within the linear range of detection. Membranes were incubated with mouse anti-Arf 1D9 and rabbit anti-GFP and were developed and analyzed. A representative western blot from four separate experiments is shown. The uncropped western blots are shown in supplementary material Fig. S1. (B) Quantification of the fold overexpression of exogenous Arf-EGFP over endogenous Arf levels was performed by comparing amount of signal in each band using Odyssey software. (C) HeLa cells were co-transfected with plasmids encoding mCherry-GBF1, myc-memrin, and either WT or T31N forms of Arf1-EGFP and imaged after fixation as for Fig. 1 ($n=3$). (D) HeLa cells were co-transfected with plasmids encoding myc-memrin and either WT or T31N forms of Arf1-EGFP as for A. Cells were then fixed and stained with mouse anti-GBF1 monoclonal antibody and imaged as for Fig. 1 ($n=3$). (E) Quantification of GBF1 recruitment in cells expressing Arf1 WT and T31N was performed by measuring the percentage of total GBF1 staining at the Golgi. Scale bars: 26 μ m.

mCherry–GBF1 and low levels of Arf1 T31N (Fig. 2C). Importantly, we observed a clear accumulation of GBF1 on Golgi membranes and dramatic loss of cytoplasmic GBF1 in cells expressing Arf1 T31N relative to those expressing WT Arf1 (Fig. 2C). Note that, although the presence of myc–membrin allowed for a higher proportion of cells with intact Golgi, it was clearly not required for the Arf1 T31N-dependent accumulation of GBF1 (supplementary material Fig. S2). More importantly, Arf1 T31N was able to induce redistribution of untagged endogenous GBF1 from the cytosol to the Golgi. Loss of cytosolic GBF1 did not result from lower expression or degradation of GBF1 in cells expressing T31N Arf1 (supplementary material Fig. S1C). The results obtained for endogenous GBF1 were quantified as a percentage of the total GBF1 signal at the Golgi and the results are shown in Fig. 2E. This analysis revealed a 3.5-fold increase in membrane associated GBF1 in T31N Arf1 transfected cells compared to WT Arf1-transfected cells (Fig. 2E). These findings provide strong evidence that Arf-GDP can regulate GBF1 localization to Golgi membranes.

GBF1 accumulates on cis-Golgi membranes in a catalytically active form

The results presented above demonstrate that GBF1 is recruited to the Golgi in response to elevated levels of its Arf-GDP substrate. This suggests a potentially novel mechanism to ensure homeostatic levels of Arf-GTP on cis-Golgi membranes by recruitment of GBF1. To assess whether GBF1 accumulated in an active form, we first determined whether the Golgi remained polarized. Current evidence suggests that the characteristic

segregation of cis- and trans-markers results from continuous Arf- and coat-dependent sorting events and requires recruitment of GBF1 to cis-Golgi membranes (Manolea et al., 2008). We first confirmed that the cis-Golgi marker p115 (also known as USO1) and trans-Golgi network marker TGN46 remained well resolved in cells expressing both inactive Arf1 T31N and myc–membrin (Fig. 3A). Although it was clear that both markers localized to the juxta-nuclear Golgi region, the patterns were clearly different (Fig. 3A), as observed in cells expressing WT Arf1 (supplementary material Fig. S3). Merging of the p115 and TGN46 panels revealed distinct red and blue signals. A line-scan analysis of a representative Golgi from the merge image in Fig. 3A confirms the significant separation observed between TGN46 (red) and p115 (blue) signal peaks (Fig. 3C). To assess whether GBF1 accumulated on cis-Golgi membranes, we repeated this analysis by comparing the distribution of endogenous GBF1 with cis-Golgi and TGN markers in cells expressing the mutant T31N Arf1 (Fig. 3B). We observed clear colocalization of endogenous GBF1 with p115 but not with TGN46. This was also confirmed by line-scan analysis (Fig. 3D).

To obtain more direct evidence that accumulated GBF1 remained active, we first determined whether COPI, a well-established effector of Arf-GTP, associated with Golgi membranes in a BFA-sensitive and therefore GBF1-dependent manner. HeLa cells were co-transfected with plasmids encoding mCherry–GBF1 and myc–membrin, as well as Arf1 T31N–EGFP to promote recruitment of GBF1. The COPI distribution was then examined in transfectants treated with either BFA or DMSO by staining for β -COP, a subunit of the COPI coat. Results

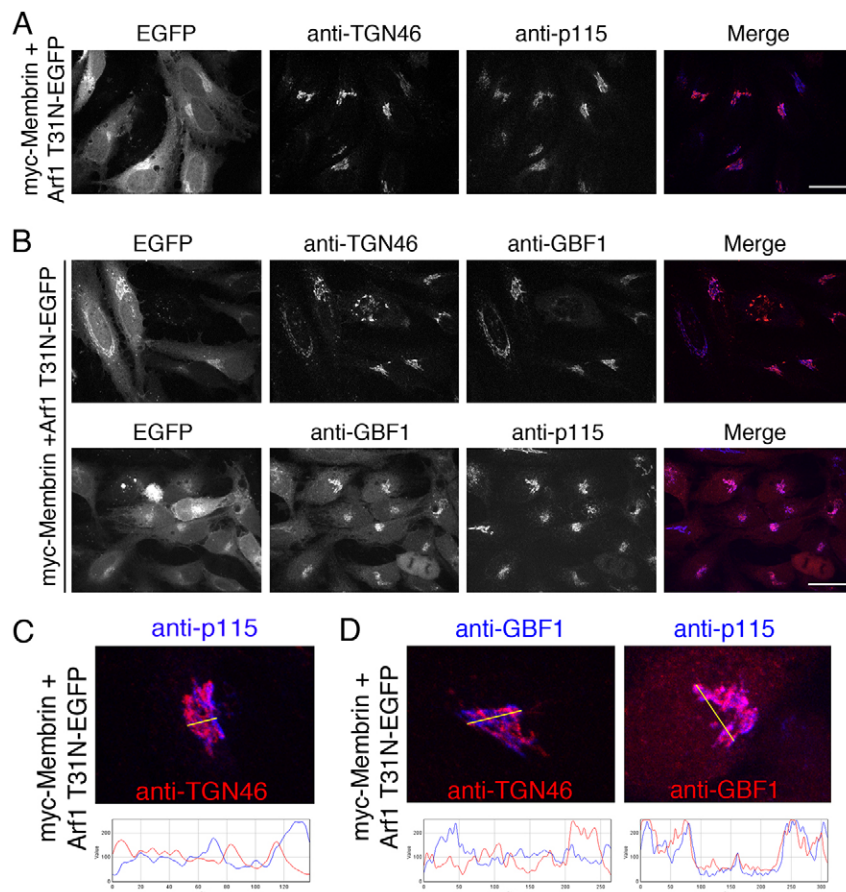


Fig. 3. Arf-GDP-dependent GBF1 accumulation does not alter Golgi polarity and GBF1 is recruited specifically to the cis-Golgi. (A) HeLa cells were co-transfected with plasmids encoding myc–membrin and Arf1 T31N–EGFP, fixed and stained with sheep anti-TGN46 and mouse anti-p115 and then imaged as for Fig. 1 ($n=3$). (B) HeLa cells were co-transfected with plasmids encoding myc–membrin and Arf1 T31N–EGFP, fixed and stained with either sheep anti-TGN46 and mouse anti-GBF1 or rabbit anti-GBF1 and mouse anti-p115 antibodies and then imaged as for Fig. 1 ($n=3$). (C) Line-scan analysis was performed on cells expressing myc–membrin and Arf1 T31N–EGFP and stained with sheep anti-TGN46 and mouse anti-p115. A magnified image of a representative Golgi from A is shown. (D) Line-scan analysis was performed on cells expressing myc–membrin and Arf1 T31N–EGFP and stained with either sheep anti-TGN46 and mouse anti-GBF1 or rabbit anti-GBF1 and mouse anti-p115 antibodies. A magnified image of a representative Golgi from B is shown. Scale bars: 26 μ m.

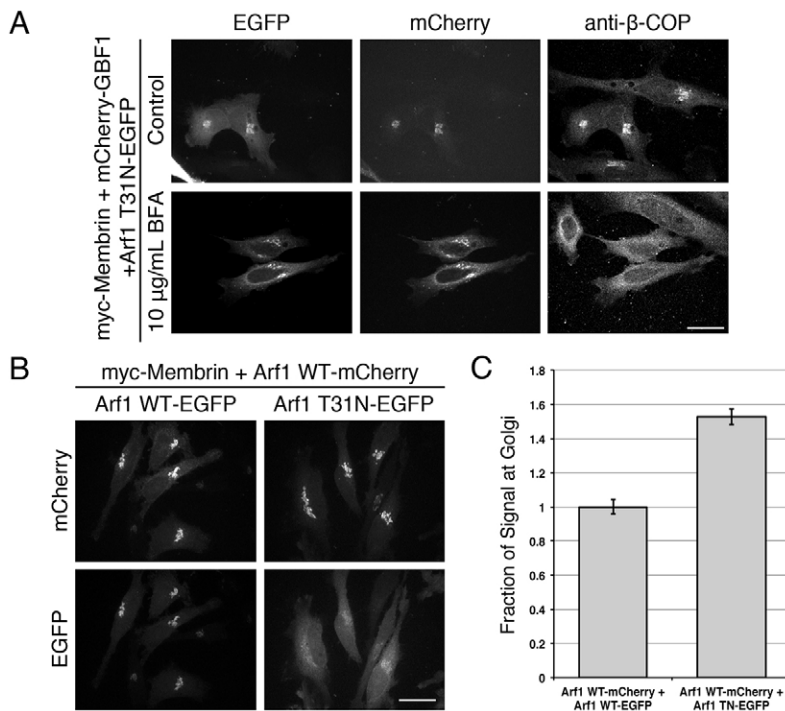


Fig. 4. GBF1 remains catalytically active following Arf-GDP-dependent recruitment. (A) HeLa cells were co-transfected with plasmids encoding myc-membrin and Arf1 T31N-EGFP and treated with either 10 µg/ml BFA or DMSO control for 20 minutes then fixed and stained with mouse anti-β-COP and imaged as for Fig. 1. Low expression of inactive Arf led to GBF1 accumulation in every cell analyzed ($n=48$) and we therefore expect all Arf-GFP-expressing cells to accumulate GBF1. COPI recruitment in cells overexpressing the WT form of Arf1 are shown in supplementary material Fig. S4. (B) Live HeLa cells expressing myc-membrin, Arf1 WT-mCherry, and either the WT or T31N form of Arf1-EGFP were imaged as for Fig. 1. (C) Quantification of the fraction of Arf1 WT-mCherry signal at the Golgi in cells expressing Arf1 T31N-EGFP was performed and normalized to cells expressing Arf1 WT-EGFP. A minimum of two cells similar to those shown in B were quantified in each of four separate experiments. Images shown in B were extracted from the experiments shown in supplementary material Fig. S6B,C. Scale bars: 26 µm.

established that a large fraction of COPI associates with juxtannuclear membranes in the presence of Arf1 T31N (Fig. 4A). Significantly, BFA treatment completely dispersed COPI (Fig. 4A, right panels), suggesting that accumulated GBF1 was active and remained sensitive to BFA.

To directly establish that recruitment of GBF1 leads to elevated Arf activation on Golgi membranes, we quantified the levels of Arf1 WT-mCherry on Golgi membranes in cells coexpressing either WT or the T31N mutant forms of Arf1-EGFP. Previous work has established that Arf association with membranes is an indirect measure of Arf activation because treatments that block Arf nucleotide exchange result in rapid redistribution of Arf to the cytosol (Donaldson et al., 1992; Helms and Rothman, 1992). The experimental set up and predicted results are illustrated in supplementary material Fig. S5. We first confirmed that GBF1 accumulates on Golgi membranes in cells coexpressing both WT and mutant Arf1 (supplementary material Fig. S6A). Live-cell imaging clearly indicated that Arf1 WT-mCherry was efficiently activated and associated with the Golgi whether the cells coexpressed WT or mutant Arf1-EGFP (Fig. 4B). In contrast, T31N Arf1-EGFP associated weakly with membranes. Most of the WT Arf1 dispersed in response to BFA treatment, leaving a small fraction on Golgi membranes, similar to that observed for the T31N mutant form of Arf1 (supplementary material Fig. S6B–D). As expected, if accumulated GBF1 is active, we observed a decrease in cytosolic WT Arf1-mCherry in cells expressing T31N Arf1-EGFP relative to those expressing WT Arf1-EGFP (Fig. 4B). This observation suggests greater Arf1 activation and association with membranes in cells containing accumulated GBF1. Quantification of several experiments similar to that in Fig. 4B revealed that there was a 50% increase in active membrane-associated Arf in cells expressing low levels of inactive Arf (Fig. 4C). This result is not only conclusive evidence that GBF1 remains active following recruitment, but also suggests that recruitment of GBF1 directly increases the amount of Arf activation at the Golgi.

Arf-GDP-dependent recruitment of GBF1 does not require PtdIns4P

The recent demonstration that PtdIns4P, through the activity of PI4KIII α , is required for the association of GBF1 with cis-Golgi membranes suggests a readily testable mechanism in which increases in Arf-GDP could result in recruitment of GBF1 by elevating levels of PtdIns4P (Dumaresq-Doiron et al., 2010). To test this possibility, we utilized a chimera containing the PtdIns4P-binding PH domain of (EYFP-PH^{FAPP}) to visually monitor intracellular PtdIns4P levels (Godí et al., 2004; De Matteis and Luni, 2008). The best-characterized approach to rapidly increase Arf-GDP is BFA treatment, which allowed us to simultaneously monitor relative changes in GBF1 and PtdIns4P levels by live-cell imaging. HeLa cells coexpressing mCherry-GBF1 and EYFP-PH^{FAPP} were treated with BFA and changes in GBF1 and PtdIns4P levels at Golgi membranes were monitored. As expected, treatment with the carrier DMSO had no impact on the distribution of either GBF1 or EYFP-PH^{FAPP} (supplementary material Fig. S7). Treatment with BFA caused the expected recruitment of GBF1 to Golgi membranes, but, contrary to the prediction of the hypothesis above, caused a rapid loss of EYFP-PH^{FAPP} from Golgi membranes (Fig. 5A).

BFA inhibits both the cis-Golgi-localized GBF1 and the TGN-localized BIGs (Sáenz et al., 2009). To more specifically assess a potential role for PtdIns4P on cis membranes where GBF1 is localized, we turned to the more selective drug Golgicide A (GCA). The bulkier GCA inhibits GBF1 activity but is excluded from the BIGs' binding site (Sáenz et al., 2009). GCA treatment of HeLa cells coexpressing mCherry-GBF1 and EYFP-PH^{FAPP} caused obvious recruitment of GBF1 on Golgi membranes (Fig. 5B). However, despite this clear increase in GBF1 signal there was no change in the EYFP-PH^{FAPP} intensity in all replicate experiments suggesting that PtdIns4P levels remained constant. The dramatic decrease in PtdIns4P levels observed following BFA treatment (Fig. 5A) probably results from inhibition of BIGs activity, as could be predicted from the well-established localization of PtdIns4P (D'Angelo et al., 2008;

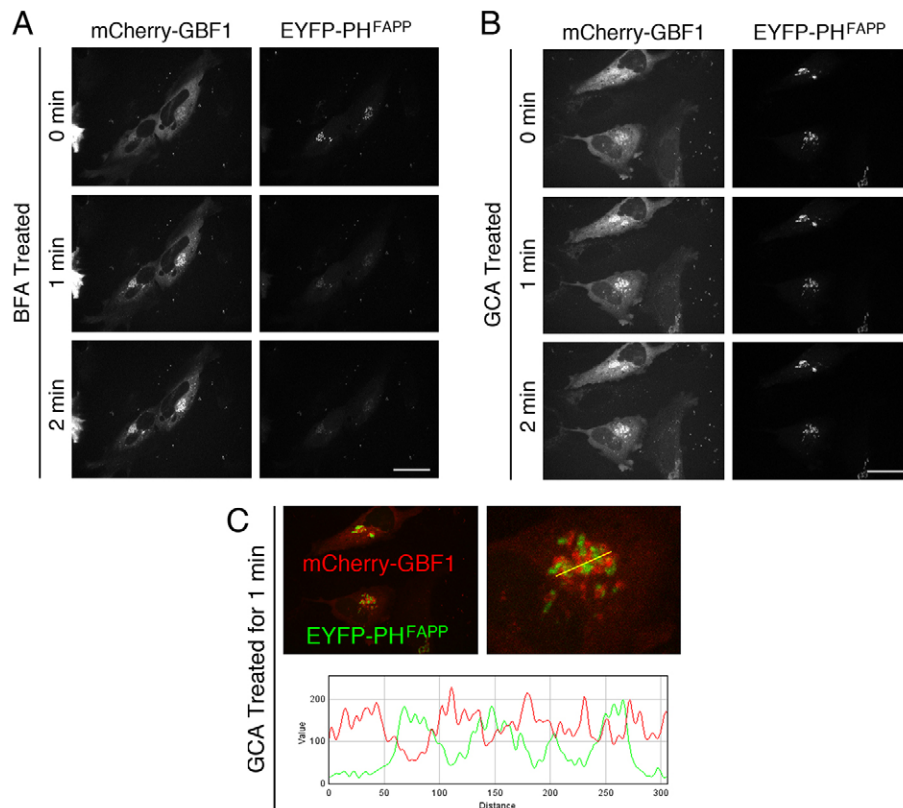


Fig. 5. Arf-GDP-dependent GBF1 recruitment to cis-Golgi membranes is independent of PtdIns4P levels. (A) HeLa cells expressing mCherry-GBF1 and EYFP-PH^{FAPP} were treated with 5 μg/ml BFA and imaged by live cell spinning disc confocal microscopy ($n=6$). (B) Live HeLa cells expressing mCherry-GBF1 and EYFP-PH^{FAPP} were treated with 10 μM GCA and imaged as for Fig. 1 ($n=6$). (C) Line-scan analysis was performed on images of cells expressing mCherry-GBF1 and EYFP-PH^{FAPP} obtained following a 1-minute treatment with 10 μM GCA. Merge image and fourfold magnification of a representative Golgi from B are shown. Scale bars: 26 μm.

Bankaitis et al., 2012) and BIGs (Shinotsuka et al., 2002; Zhao et al., 2002; Manolea et al., 2008) to the TGN. This interpretation is further supported by our observation that accumulated mCherry-GBF1 is well-resolved from EYFP-PH^{FAPP} (Fig. 5C). The clear separation of the GBF1 and PtdIns4P signals is most apparent in the magnified image and line-scan (Fig. 5C). Taken together, these data suggest that the mechanism by which Arf-GDP recruits GBF1 to cis-Golgi membranes is independent of the PtdIns4P level and that, contrary to previous reports, GBF1 recruitment does not require PtdIns4P for membrane binding.

Most Golgi-associated Arfs can regulate recruitment of GBF1

Experiments to date focused on the more abundant Arf1 isoform. However, all Arf isoforms but Arf6 associate to some extent with cis-Golgi membranes and must therefore be activated by GBF1 *in vivo*. For this reason, we predict that GBF1 recruitment should respond to all isoforms to maintain adequate levels of each distinct Arf isoform. To test this prediction, HeLa cells expressing mCherry-GBF1, myc-membrin and various Arf T31N-EGFP mutants were examined for accumulation of GBF1 on Golgi membranes. The left panels in Fig. 6A show the distribution of overexpressed GBF1 in cells coexpressing either class I (Arf1 or Arf3) or class II (Arf4 or Arf5) Arf mutants. Expression of inactive forms of both class I Arfs caused dramatic recruitment of GBF1 on a juxta-nuclear Golgi (Fig. 6A). Expression of T31N Arf5 caused reproducible fragmentation of the Golgi, and, in every case examined, GBF1 accumulated on the Golgi fragments. In contrast, expression of the other class II Arf, T31N Arf4, failed to cause GBF1 recruitment. These results indicate that most inactive Arf isoforms can promote GBF1 recruitment, and suggest that there is a

substrate-driven recruitment mechanism by which GBF1 can maintain active levels of all Arf isoforms at the Golgi.

Arf-GDP-dependent accumulation of GBF1 requires membrane association of Arf-GDP

Recruitment of GBF1 to the Golgi probably involves a putative compartment-specific membrane-bound receptor and regulation of its activity should occur at the membrane. To begin addressing the mechanism by which Arf-GDP recruits GBF1 to cis-Golgi membranes, we therefore examined whether association of Arf-GDP with membranes was required. Several studies have demonstrated that N-terminal myristoylation of Arf proteins is required for efficient binding to membranes because mutation of the myristoylation site from glycine to alanine (G2A) abolishes membrane binding (Franco et al., 1993; Haun et al., 1993; Kahn et al., 1995). A double mutant of inactive Arf lacking the essential myristoylation site (G2A, T31N) provided us with a tool with which to readily test our hypothesis.

HeLa cells expressing myc-membrin and low levels of either WT, T31N, or T31N, G2A forms of Arf1-EGFP were stained for endogenous GBF1 (Fig. 6B). As previously observed (Fig. 2A,B), expression of WT Arf1 failed to accumulate GBF1, whereas that of the T31N mutant led to potent recruitment of GBF1. As expected, the T31N, G2A double mutant did not associate to any detectable extent with Golgi membranes. More importantly, the T31N, G2A double mutant did not cause significant accumulation of GBF1 on Golgi membranes in any of the transfectants examined. GBF1 failed to accumulate even in cells expressing significantly higher levels of the Arf1 T31N, G2A double mutant (Fig. 6B, cell in the center of the bottom right panel). These results indicate that the membrane association of Arf-GDP is required for subsequent GBF1

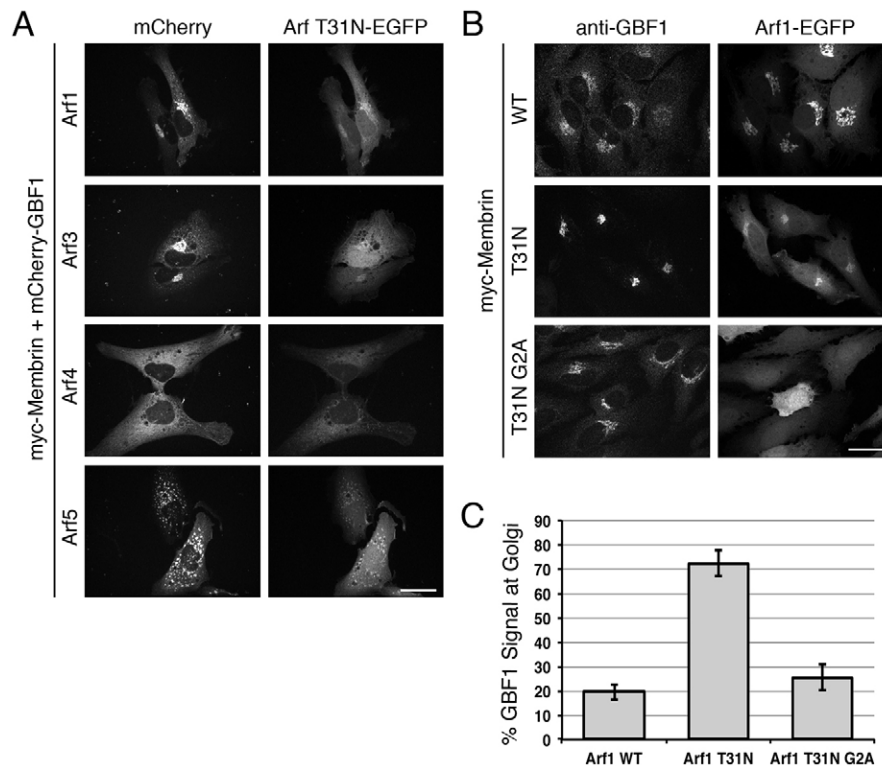


Fig. 6. Arf-GDP-dependent recruitment of GBF1 to cis-Golgi membranes is not specific to an Arf isoform and requires Arf-GDP association with Golgi membranes. (A) Live HeLa cells were co-transfected with plasmids encoding mCherry-GBF1, myc-membrin, and either EGFP-tagged Arf1, Arf3, Arf4 or Arf 5 T31N and imaged as for Fig. 1. (B) HeLa cells were co-transfected with plasmids encoding myc-membrin and Arf1 WT-EGFP, Arf1 T31N-EGFP or Arf1 T31N G2A-EGFP. Cells were then fixed and stained with mouse anti-GBF1 monoclonal antibody and imaged as for Fig. 1. (C) Quantification of GBF1 recruitment at the Golgi in cells expressing Arf1 WT, T31N, and T31N G2A was performed by measuring the percentage of total GBF1 staining at the Golgi. A minimum of eight cells similar to those shown in B were quantified in each of three separate experiments. Scale bar: 26 μ m.

recruitment. Quantification of the GBF1 signal at the Golgi from several similar experiments established that expression of T31N, G2A Arf1 did not cause a significant increase in GBF1 at the Golgi. The percentage of GBF1 signal at the Golgi in cells expressing T31N, G2A Arf1 is very similar to that observed with WT Arf1, whereas expression of T31N Arf1 caused a 3.5-fold increase in GBF1 level at the Golgi (Fig. 6C), as previously observed (Fig. 2E). In summary, these results demonstrate that the membrane association of Arf-GDP is required for subsequent recruitment of GBF1 on a cis-Golgi localized factor.

DISCUSSION

In this study, we elucidated a novel mechanism for the regulation of recruitment of GBF1 on cis-Golgi membranes. Several laboratories have previously reported that treatment with BFA causes a rapid accumulation of GBF1 on Golgi membranes, an effect attributed to formation of an Arf-BFA-GEF membrane-bound complex. We extended those results and report that several manipulations that increase Arf-GDP levels, including Exo1 treatment and ArfGAP1 overexpression, also cause accumulation of endogenous GBF1 on Golgi membranes. These results are consistent with our previous report showing that trapping of Arf on a membrane-bound GEF is not detected *in vivo* (Chun et al., 2008), and suggest instead that it is accumulation of Arf-GDP that promotes recruitment of GBF1. The possibility that Arf-GDP positively regulates GBF1 association with membranes was tested using inactive ‘GDP-arrested’ Arf T31N mutants. We found that expression of even low levels of several Arf T31N isoforms caused dramatic accumulation of GBF1 on membranes. Under these conditions, the Golgi still displayed separate cis- and trans-Golgi markers, and the Arf-GDP-dependent enrichment of GBF1 occurred selectively on cis-Golgi membranes. Moreover, the accumulated GBF1 resulted in increased Arf-GTP production

and was therefore active. Accumulation of GBF1 on Golgi membranes occurred independently of PtdIns4P levels. Arf-GDP-dependent recruitment of GBF1 depended on the myristoylation of the Arf N-terminal helix that is required for membrane association. Our results suggest Arf-GDP-dependent regulation of a membrane-associated factor for recruitment of GBF1 that is located specifically on cis-Golgi membranes.

GBF1 is recruited to Golgi membranes in response to increases in Arf-GDP

It has been hypothesized (Niu et al., 2005; Szul et al., 2007) that treatment of cells with BFA results in accumulation of GBF1 on Golgi membranes due to the formation of an ‘abortive complex’, first observed biochemically *in vitro* using purified components (Béraud-Dufour et al., 1998; Peyroche et al., 1999; Renault et al., 2003). More recently, our laboratory tested this hypothesis and found no coincident recruitment of GBF1 and Arf to Golgi membranes following BFA treatment (Chun et al., 2008). This result suggested that BFA inhibition *in vivo* induces a physiological response resulting in GBF1 recruitment to Golgi membranes in a form that no longer binds Arf to form a stable Arf-BFA-GBF1 complex. In this study, we further tested the hypothesis and discovered that various treatments that decrease Arf-GTP, resulting in a corresponding increase in Arf-GDP, cause GBF1 recruitment and accumulation. For example, as shown in Fig. 1, overexpression of active ArfGAP1 led to a clear accumulation of GBF1 on Golgi membranes. In contrast, expression of an inactive mutant ArfGAP1 caused significant reduction of GBF1 recruitment to Golgi membranes compared to control cells, suggesting that this mutant interferes with Arf-GTP hydrolysis and thus the production of Arf-GDP. This, in turn, results in a lesser requirement for GBF1 to produce Arf-GTP, which is achieved by lower levels of recruited GBF1.

As predicted, expression of even very low levels of the inactive T31N mutant of several Arfs was sufficient to induce the recruitment and accumulation of both overexpressed and endogenous GBF1 (Fig. 2). To further define the mechanism by which Arf-GDP promotes GBF1 recruitment to membranes we assessed if a specific Golgi-associated Arf isoform played a regulatory role. These experiments established that expression of inactive mutants of Arf1, Arf3, and Arf5 caused GBF1 accumulation on Golgi membranes; only Arf4 T31N failed to do so (Fig. 6). Arf4 T31N does not disrupt the Golgi and might not properly mimic the GDP-bound form. We expect that the true GDP-bound form of all class I and class II Arfs can regulate the recruitment of GBF1. Our results suggest that GBF1 has evolved to respond equally to the production of most Golgi-associated Arf species.

The experiments discussed above led us to propose that Arf-GDP plays a regulatory role by activating a putative GBF1 receptor found specifically on membranes of the cis-Golgi and ERGIC (Fig. 7). In this model, cells can monitor levels of Arf-GDP at the membrane and respond by adjusting GBF1 recruitment to cis-Golgi membranes in order to maintain homeostasis by nucleotide exchange. Several lines of evidence discussed below support the possibility that accumulation of Arf-GDP promotes selective recruitment of active GBF1 on cis-Golgi membranes.

GBF1 enriched on membranes remains catalytically active and maintains Golgi polarity and function

For our model to be physiological relevant, Arf-GDP-dependent recruitment of GBF1 must result in increased GBF1 activity at the cis-Golgi. Specifically, we would expect to observe selective recruitment of GBF1 to membranes of the early secretory pathway, as well as subsequent Arf activation and maintenance of a polarized Golgi. Under conditions that caused GBF1 enrichment, we indeed observed that GBF1 was recruited specifically to cis-Golgi membranes on a Golgi that remained polarized with clearly resolved cis-Golgi and TGN elements (Fig. 3). The activity of accumulated GBF1 was confirmed by the dual observations that COPI was efficiently recruited to Golgi structures and that elevated GBF1 levels yielded 50% greater Arf activation relative to control conditions (Fig. 4). As expected if COPI and Arf membrane association required GBF1 activity, COPI recruitment

and Arf activation remained BFA-sensitive in each assay (Fig. 4). These data establish that Arf-GDP-dependent recruitment of GBF1 occurs specifically on cis-Golgi membranes, results in GBF1 activity, and demonstrate a novel and physiologically relevant model for regulation of GBF1 recruitment.

Arf-GDP must be membrane-associated to regulate recruitment of GBF1 to membranes

To examine the mechanism through which Arf-GDP regulates GBF1 recruitment we first examined its potential involvement in modulating PtdIns4P levels using the well-characterized biosensor EYFP-PH^{FAPP} (Godi et al., 2004; De Matteis and Luini, 2008). This hypothesis was based on a report by LeFrancois and colleagues suggesting that production of PtdIns4P was required for recruitment of GBF1 to Golgi membranes (Dumaresq-Doiron et al., 2010). However, experiments involving treatment with BFA or GCA revealed no correlation between GBF1 recruitment and PtdIns4P levels (Fig. 5). Treatment with BFA, which targets both GBF1 and BIGs, caused GBF1 accumulation and almost complete loss of the PtdIns4P signal from the Golgi. In contrast, treatment with the GBF1-specific inhibitor GCA also caused GBF1 accumulation but had no impact on PtdIns4P levels. More importantly, GBF1 recruitment occurred on membranes that appeared clearly distinct from membranes positive for PtdIns4P. Whereas those experiments failed to reveal a link between GBF1 and PtdIns4P, they established a predicted but as yet uncharacterized link between the production of the TGN-localized PtdIns4P (Odorizzi et al., 2000; De Matteis et al., 2005; D'Angelo et al., 2008) and the BFA-sensitive but GCA-resistant BIGs, also localized at the TGN (Shinotsuka et al., 2002; Zhao et al., 2002; Manolea et al., 2008). Furthermore, these results confirm that GBF1 localization occurs primarily on cis-Golgi membranes (Kawamoto et al., 2002; Zhao et al., 2002).

As an alternative to the candidate approach summarized above, we turned to the more basic question of whether Arf-GDP must be membrane-associated to regulate recruitment of GBF1 to membranes. Two plausible mechanisms appeared reasonable. Arf-GDP could interact with its target in cytoplasm, possibly GBF1 itself, to modulate its affinity for the membrane. Alternatively, Arf-GDP could interact with its target at the

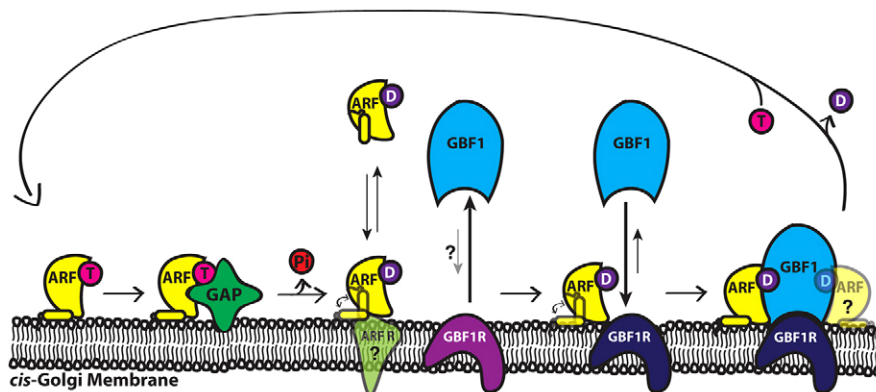


Fig. 7. Diagram depicting the novel 'Arf-GDP increase' model for regulation of GBF1 recruitment to cis-Golgi membranes. Arf-GDP acts as a trigger for GBF1 recruitment. Regulatory Arf-GDP can arise through hydrolysis of Arf-GTP by its GAP or can be recruited directly from cytosol to a no- or low-affinity receptor (magenta) that likely requires Arf-GDP for activation (dark blue). The nature of the binding site for regulatory Arf-GDP remains unknown but must be at the membrane, possibly the GBF1 receptor itself. However, we cannot eliminate the possibility that Arf-GDP is regulating a lipid-modifying enzyme to cause GBF1 recruitment. This self-limiting model provides a mechanism to maintain homeostatic levels of Arf-GTP. T, GTP; D, GDP; Pi, inorganic phosphate.

membrane, possibly a putative GBF1 receptor, to modulate its affinity for GBF1. Such information not only helps define the regulatory mechanism but also provides avenues for identification of putative receptors. To distinguish between these two potential mechanisms, we took advantage of a well-characterized Arf G2A mutation that abrogates myristoylation of the N-terminal helix of Arf, which is required for its membrane association (Franco et al., 1993; Haun et al., 1993; Kahn et al., 1995). As shown in Fig. 6, expression of the Arf1 T31N G2A double mutant failed to induce GBF1 recruitment, even in cells overexpressing the putative Arf-GDP receptor, membrin. These results demonstrate that myristate-dependent membrane association of Arf-GDP is required to elicit recruitment of GBF1, potentially to an unknown cis-Golgi-bound factor.

Arf-GDP-dependent recruitment of GBF1 to cis-Golgi membranes is likely to establish and maintain homeostatic levels of Arf-GTP

ArfGEF recruitment to membranes is a crucial step in initiating guanine nucleotide exchange on Arf proteins at the Golgi (Paris et al., 1997). Our model for the regulation of GBF1 recruitment to cis-Golgi membranes centers on the response of the cell to changes in Arf-GDP levels (Fig. 7). This model accounts for our observation that increasing Arf-GDP levels promotes GBF1 membrane association, whereas decreasing Arf-GDP levels results in reduced GBF1 association with membranes. More importantly, this self-limiting model provides a simple mechanism to maintain homeostatic levels of Arf-GTP. Indeed, increases in the substrate Arf-GDP promote recruitment of GBF1 and subsequent Arf activation. Conversely, ongoing activation eventually leads to a local reduction in Arf-GDP levels that decreases GBF1 recruitment and establishes the desired steady-state level of Arf-GTP. Stimulation of ArfGEF recruitment by Arf-GTP has been previously reported for members of the BIG (Richardson and Fromme, 2012; Richardson et al., 2012; Lowery et al., 2013) and cytohesin families (Cohen et al., 2007; Hofmann et al., 2007). The mechanism reported here for GBF1 appears new because it involves Arf-GDP.

The model also takes into account our demonstration that association of Arf-GDP with membranes is crucial for regulation (Fig. 6). Such results suggest the presence of a membrane-associated target, either a non-catalytic domain of GBF1 or possibly the GBF1 receptor itself. Whether Arf-GDP simply increases the affinity of GBF1 for the membrane or its receptor, or is actually required for its activation remains unknown. Our observation that overexpression of the GAP-dead mutant, which will reduce production of Arf-GDP, leads to near elimination of GBF1 recruitment (Fig. 1D), suggests that the GBF1 receptor has no or extremely low affinity for GBF1 in absence of Arf-GDP.

Our data allows us to also speculate on the regulation of ArfGAP1, whose activity opposes that of GBF1 at cis-Golgi membranes. Previous studies have reported that the expression of catalytically dead mutants of ArfGAP1 did not lead to observable phenotypes on the Golgi (Liu et al., 2005). Our data can now explain this unexpected result through modulation of GBF1 recruitment. For example, expression of the ArfGAP1 R50Q mutant decreases GBF1 recruitment by roughly 50% (Fig. 1D,E), thereby reducing Arf-GTP production and probably compensating for the loss of ArfGAP activity. In other words, our results suggest that cells adjust GBF1 recruitment to correct for decreased GAP activity. Cells could establish homeostatic Arf-GTP levels by regulating GAP and/or GEF activity. Our results also suggest that cells do not readily modulate endogenous GAP activity. This conclusion is based on the fact that accumulation of GBF1 to Golgi

membranes results in a 50% greater activation of Arf (Fig. 4B,C), and therefore appears not to be compensated for by increased GAP activity. Together these results suggest that whereas the GEF is extremely sensitive to alterations in Arf-GTP:Arf-GDP ratio, the GAP appears to be largely unresponsive.

Concluding remarks

The work described here yielded novel insights into how BFA acts *in vivo*, identified a new mechanism of GBF1 recruitment regulation, and for the first time attributed a role for Arf-GDP in the cell. The work also provides us with tools that should lead to the identification of the putative GBF1 receptor. The recruitment of GBF1, as proposed for other GEFs (Richardson et al., 2012), could respond simultaneously to several stimuli such as phosphoinositide level, Rab1 (Alvarez et al., 2003) and receptor abundance and/or modification. Current work towards identification of a receptor will greatly add to our understanding of GBF1 function and could potentially lead to the discovery of therapeutics for the treatment of diseases resulting from GBF1 dysfunction and those caused by viruses that manipulate GBF1 function and localization to ensure successful replication.

MATERIALS AND METHODS

Reagents and antibodies

Exo1 was purchased from Calbiochem (Gibbstown, NJ) and stored in DMSO as a 100 mM stock. BFA and GCA were purchased from Sigma-Aldrich (St. Louis, MO) and stored in DMSO at 10 μ g/ml and 10 mM, respectively. Monoclonal antibodies used for immunofluorescence were mouse anti-GBF1 (clone 25; BD Biosciences, Mississauga, ON), mouse anti- β -coatomer protein I (COPI) (clone m3a5; Sigma-Aldrich), and mouse anti-p115 (7D1; gift from the late Dennis Shields, Albert Einstein College of Medicine, NY). Polyclonal antibodies used for immunofluorescence were sheep anti-TGN46 (AbD Serotec, Oxford, UK) and rabbit anti-GBF1 (9D4 final bleed; Manolea et al., 2008). Secondary antibodies used were Alexa-Fluor-647-conjugated goat anti-mouse, Alexa-Fluor-555-conjugated donkey anti-sheep, and Alexa-Fluor-546-conjugated goat anti-rabbit (Invitrogen, Carlsbad, CA) at 1:600. Antibodies used for western blotting were rabbit polyclonal anti-GFP (Eusera, Edmonton, AB) at 1:50,000 and mouse monoclonal anti-Arf (1D9; Abcam, Cambridge, MA) at 1:500. Secondary antibodies used for western blotting were Alexa-Fluor-750-conjugated goat anti-rabbit and Alexa-Fluor-680 conjugated goat anti-mouse (Invitrogen, Carlsbad, CA) at 1:10,000.

Cell culture

HeLa cells were from ECACC (Porton Down, UK). HeLa cells were cultured in DMEM containing high glucose and 2 mM L-glutamine and supplemented with 10% fetal bovine serum (Sigma-Aldrich) and 100 μ g/ml penicillin and streptomycin at 37°C in a 5% CO₂ incubator. Transfections were performed using TransIT-2020 transfection reagent or TransIT LTI transfection reagent (Mirus Bio, Madison, WI). For experiments involving co-transfection, we performed a series of preliminary experiments in which we compared the relative expression levels using various ratios of plasmids. These experiments identified optimal conditions to obtain balanced expression.

Construction and expression of plasmids

The construction of the plasmids encoding Arf1, Arf3, Arf4, and Arf5 tagged with either GFP or mCherry has been previously described (Chun et al., 2008). The Arf4 T31N, G2A double mutant was created by site-directed mutagenesis using the QuikChange kit (Stratagene, La Jolla, CA), as per the manufacturer's instructions. The plasmid encoding myc-membrin (Hay et al., 1997) was a gift from J. Hay (Division of Biological Sciences, University of Montana, Missoula, MT). The plasmid encoding EYFP-PH^{FAPP} (Godí et al., 2004) was obtained through S. Grinstein (Sick Kids, ON). Construction of a plasmid encoding ArfGAP1 tagged with EGFP at the N-terminus was as previously described (Pamis et al., 2006). A point mutant lacking GAP activity (EGFP-GAP1 R50Q) was created by site-directed mutagenesis using the QuikChange kit (Stratagene, La Jolla, CA).

Immunofluorescence and live-cell time-lapse imaging

For live-cell imaging, cells were grown on #1D round coverslips (Fisher Scientific, Ottawa, ON). Immediately before imaging, coverslips were transferred to an Atofluor live cell chamber (Invitrogen) and CO₂-independent medium (Invitrogen) supplemented with 10% fetal bovine serum was added. Image analysis was only performed on transfectants displaying intact Golgi and low levels of the proteins of interest. Imaging was performed on the temperature controlled (37°C) stage of an Axiovert 200M confocal microscope (Carl Zeiss, Thornwood, NY) equipped with an UltraVIEW ERS 3E spinning disc (PerkinElmer Life and Analytical Sciences, Waltham, MA) and a 63× objective lens (plan-Apochromat, NA 1.4) heated by an objective warmer set to 35°C. Live-cell imaging was performed in a room maintained at 26°C. Images were captured with a 9100-50 electron multiplier charge-coupled device digital camera (Hamamatsu Photonics, Bridgewater, NJ) and acquired using Velocity software (PerkinElmer Life and Analytical Sciences). Live-cell experiments with dual labeling were imaged by exciting each fluorophore and detecting sequentially before moving to the next z-slice to avoid bleed through. Laser intensity, filters, and camera gain were optimized to provide maximal signal without saturation or bleaching. When stated, drugs were introduced by addition of 250 µl of CO₂-independent medium containing 6× concentration of the drug to be tested to the Atofluor chamber containing 1.25 ml medium. Addition of drug caused a slight shift in focus at the time of addition, but this corrected itself for subsequent time points.

Imaging of fixed cells was performed using HeLa cells grown on square coverslips (Corning Life Sciences, Tewksbury, MA). Drug treatments were performed at 37°C. Coverslips were then washed with phosphate-buffered saline (PBS), and fixed with 3% paraformaldehyde in PBS at 37°C for 15 minutes. Cells were washed and permeabilized with 0.1% Triton X-100 (Sigma) in PBS and subsequently stained with antibodies. Coverslips were mounted on slides using ProLong Gold anti-fading reagent with DAPI (Invitrogen) mounting medium and allowed to dry before imaging by spinning disc confocal microscopy, as described above, without heating.

Image quantification and analysis

Quantification of ratio of Golgi signal to cytosolic signal and the percentage signal at the Golgi was performed using Imaris ×64 version 7.4.2 software (Bitplane AG, South Windsor, CT). Regions of interest were surface-wrapped in three-dimensions utilizing the surfaces option and average pixel intensities of the Golgi and cell, and were exported to Excel (Microsoft, Redmond, WA). Golgi and cell mean intensity values were corrected for cytosolic or background contributions, respectively. For fixed cell experiments, at least eight cells were quantified from three separate experiments for each condition. For live-cell experiments, at least eight cells were quantified from a total of four individual experiments. All graphs were generated in Excel. Error bars represent the standard deviation in the samples quantified. Normalization in Fig. 4C was performed by taking the average of the four pre-treatment time points and normalizing that value to 1 for each condition. In Fig. 4D, the Arf1 WT and Arf1 T31N average values were normalized to the average starting value of Arf1 WT and compared.

Preparation of cell extracts, western blots, and analysis

HeLa cells were grown on 10-cm plates to ~80–90% confluency. Cells were transfected by TransIt-2020 reagent (Mirus Bio) with 1.4 µg pCMV-myc-membrin and 1.75 µg pEGFP-Arf1 WT or T31N DNA for 18–20 hours. Transfection efficiency of Arf plasmids was estimated to be ~80–90%. Cells were released in presence of 0.25% trypsin (Invitrogen) and then collected by centrifugation. Pelleted cells were washed once in PBS and then resuspended in 1 ml 0.5% Triton X-100 (Sigma) lysis buffer (1% Triton X-100, 150 mM NaCl, and 50 mM Tris-HCl pH 8.0) containing EDTA-free protease inhibitor cocktail (Roche) and incubated on a rotator for 1 hour to allow complete lysis. Nuclei and debris were subsequently removed by centrifugation at 9300 g at 4°C. Resulting supernatant was then transferred to a fresh tube and precipitated by addition of 5× volumes of –20°C acetone and incubation at –20°C for a minimum of 4 hours. Precipitated proteins were recovered by centrifugation at 11,200 g for 10 minutes at 4°C. The resulting pellets

were air dried and resuspended thoroughly in 50 µl lysis buffer and 10 µl 6× loading buffer containing DTT (360 mM Tris-HCl pH 6.8, 60% glycerol, 12% SDS, 0.6% Bromophenol Blue and 600 mM DTT). Samples were boiled for 10 minutes at 100°C, and separated by Tris-glycine SDS-PAGE on 12% gels using protein standards (Bio-Rad).

To assess relative Arf overexpression, we performed quantitative western blot analysis. After electrophoresis, proteins were transferred onto nitrocellulose membranes (GE Healthcare, Chalfont St Giles, UK), immunoblotted with primary antibodies raised against Arf and GFP followed by Alexa-Fluor-680- and Alexa-Fluor-750-conjugated (Invitrogen) secondary antibodies. Bands were subsequently detected by Odyssey Li-Cor scanner and quantified using application software version 3.0.21. Band intensity quantification was performed using the 10 µl-loaded lanes from four individual experiments.

Acknowledgements

We thank A. Simmonds (University of Alberta, AB) for technical help with confocal microscopy and secondary antibodies. We also thank P. LaPointe, R. Lehner, N. Touret and R. Wozniak (University of Alberta, AB) for helpful discussions. We thank J. Hay (University of Montana, MT), S. Grinstein (Hospital For Sick Children, ON) for gifts of plasmids encoding myc-membrin and EYFP-PH^{FAPP}, respectively.

Competing interests

The authors declare no competing interests.

Author contributions

D.Q. performed all experiments; F.G. and N.S. generated plasmids and/or performed preliminary experiments; D.C. provided ArfGAP plasmids; P.M. and D.Q. conceived the project, analysed data, designed the figures and wrote the manuscript with comments from co-authors.

Funding

This study was supported by an operating grant to P.M. from the Canadian Institutes of Health Research [grant numbers FRN 107519, FRN 111028], the Israel Science Foundation [grant number 37/11 to D.C.]; and scholarships to D.Q. from the Faculty of Medicine and Dentistry and the Faculty of Graduate Studies and Research at the University of Alberta.

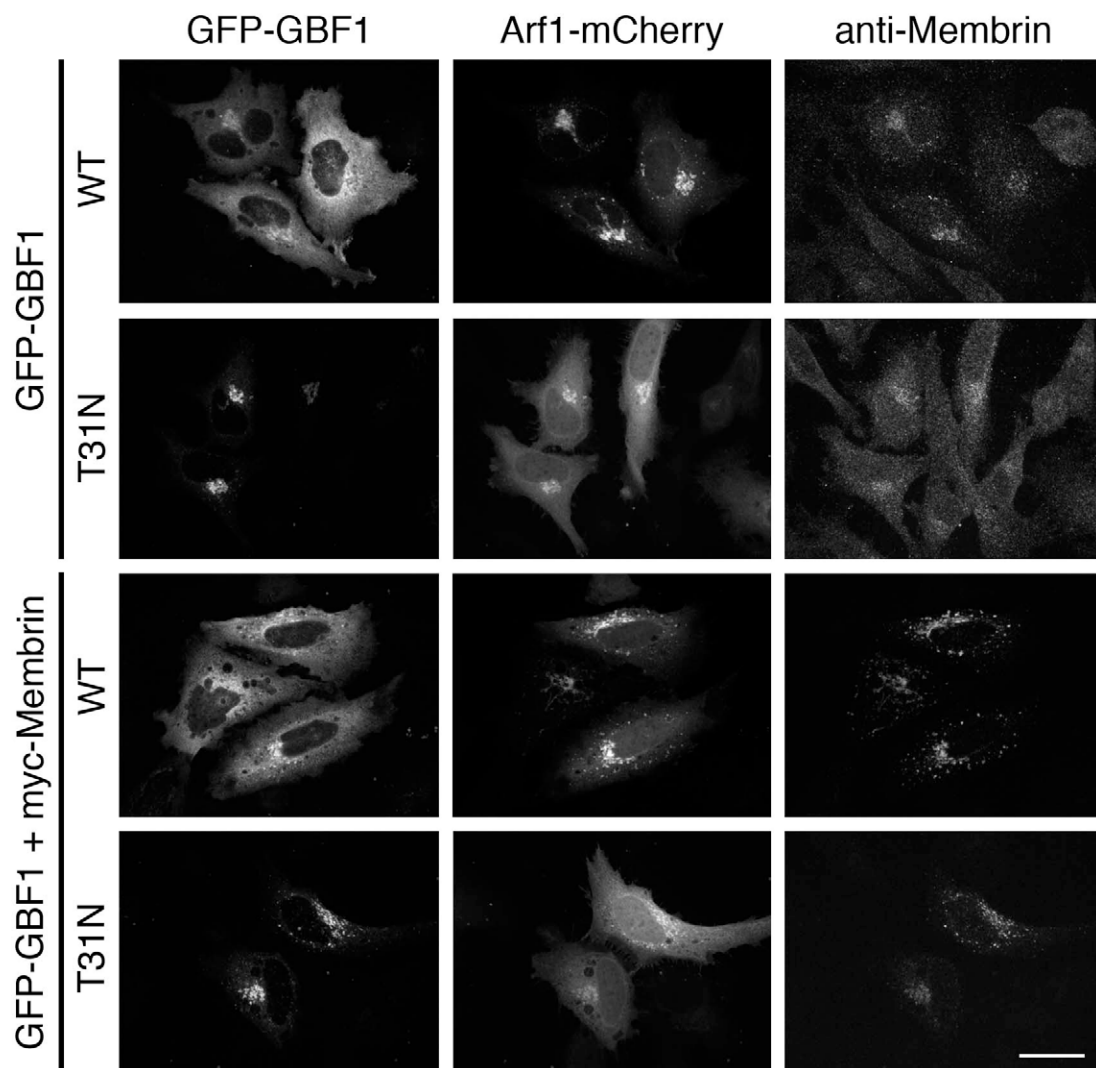
Supplementary material

Supplementary material available online at <http://jcs.biologists.org/lookup/suppl/doi:10.1242/jcs.130591/-DC1>

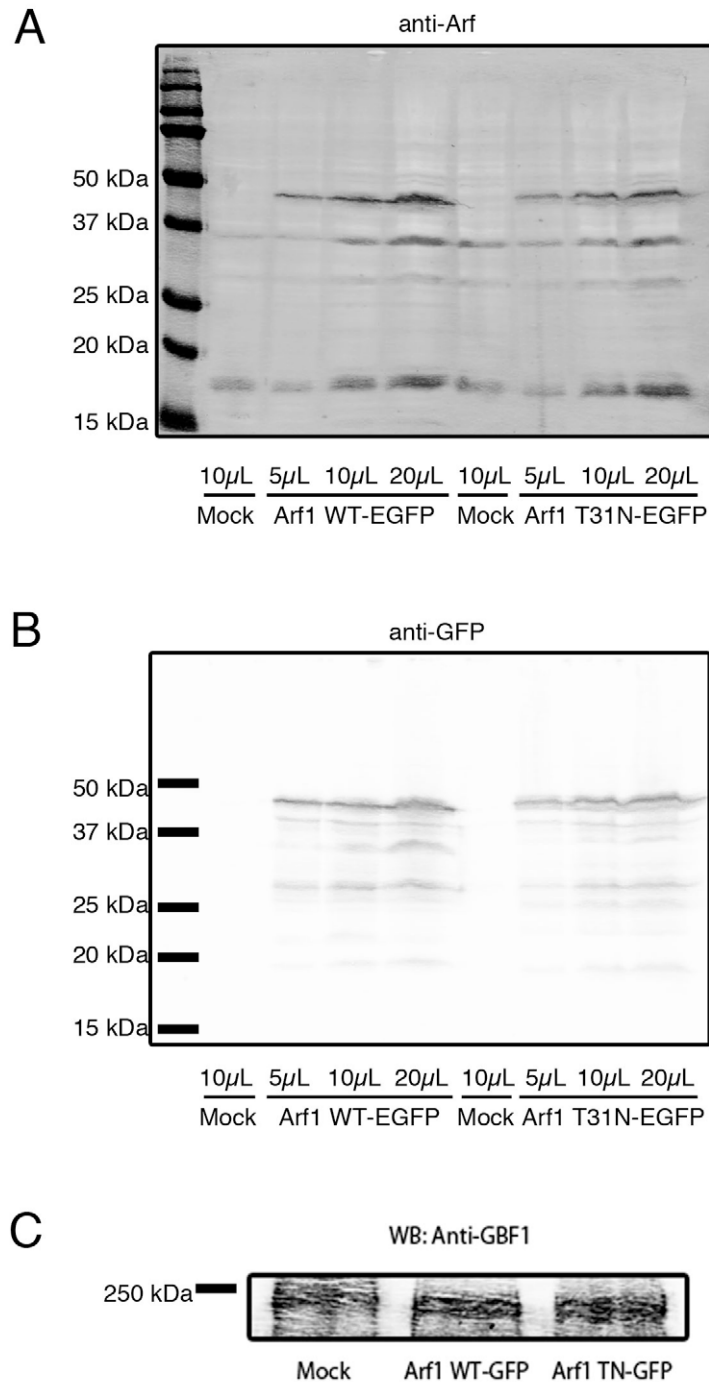
References

- Alvarez, C., Garcia-Mata, R., Brandon, E. and Sztul, E. (2003). COPI recruitment is modulated by a Rab1b-dependent mechanism. *Mol. Biol. Cell* **14**, 2116–2127.
- Bankaitis, V. A., Garcia-Mata, R. and Mousley, C. J. (2012). Golgi membrane dynamics and lipid metabolism. *Curr. Biol.* **22**, R414–R424.
- Béraud-Dufour, S., Robineau, S., Chardin, P., Paris, S., Chabre, M., Cherfils, J. and Antony, B. (1998). A glutamic finger in the guanine nucleotide exchange factor ARNO displaces Mg²⁺ and the beta-phosphate to destabilize GDP on ARF1. *EMBO J.* **17**, 3651–3659.
- Casanova, J. E. (2007). Regulation of Arf activation: the Sec7 family of guanine nucleotide exchange factors. *Traffic* **8**, 1476–1485.
- Cherfils, J. and Melançon, P. (2005). On the action of Brefeldin A on Sec7-stimulated membrane-recruitment and GDP/GTP exchange of Arf proteins. *Biochem. Soc. Trans.* **33**, 635–638.
- Chun, J., Shapovalova, Z., Dejgaard, S. Y., Presley, J. F. and Melançon, P. (2008). Characterization of class I and II ADP-ribosylation factors (Arfs) in live cells: GDP-bound class II Arfs associate with the ER-Golgi intermediate compartment independently of GBF1. *Mol. Biol. Cell* **19**, 3488–3500.
- Claude, A., Zhao, B. P., Kuziemy, C. E., Dahan, S., Berger, S. J., Yan, J. P., Arnold, A. D., Sullivan, E. M. and Melançon, P. (1999). GBF1: A novel Golgi-associated BFA-resistant guanine nucleotide exchange factor that displays specificity for ADP-ribosylation factor 5. *J. Cell Biol.* **146**, 71–84.
- Cohen, L. A., Honda, A., Varnai, P., Brown, F. D., Balla, T. and Donaldson, J. G. (2007). Active Arf6 recruits ARNO/cytohesin GEFs to the PM by binding their PH domains. *Mol. Biol. Cell* **18**, 2244–2253.
- Cukierman, E., Huber, I., Rotman, M. and Cassel, D. (1995). The ARF1 GTPase-activating protein: zinc finger motif and Golgi complex localization. *Science* **270**, 1999–2002.
- D'Angelo, G., Vicinanza, M., Di Campli, A. and De Matteis, M. A. (2008). The multiple roles of PtdIns(4)P — not just the precursor of PtdIns(4,5)P₂. *J. Cell Sci.* **121**, 1955–1963.
- Dascher, C. and Balch, W. E. (1994). Dominant inhibitory mutants of ARF1 block endoplasmic reticulum to Golgi transport and trigger disassembly of the Golgi apparatus. *J. Biol. Chem.* **269**, 1437–1448.

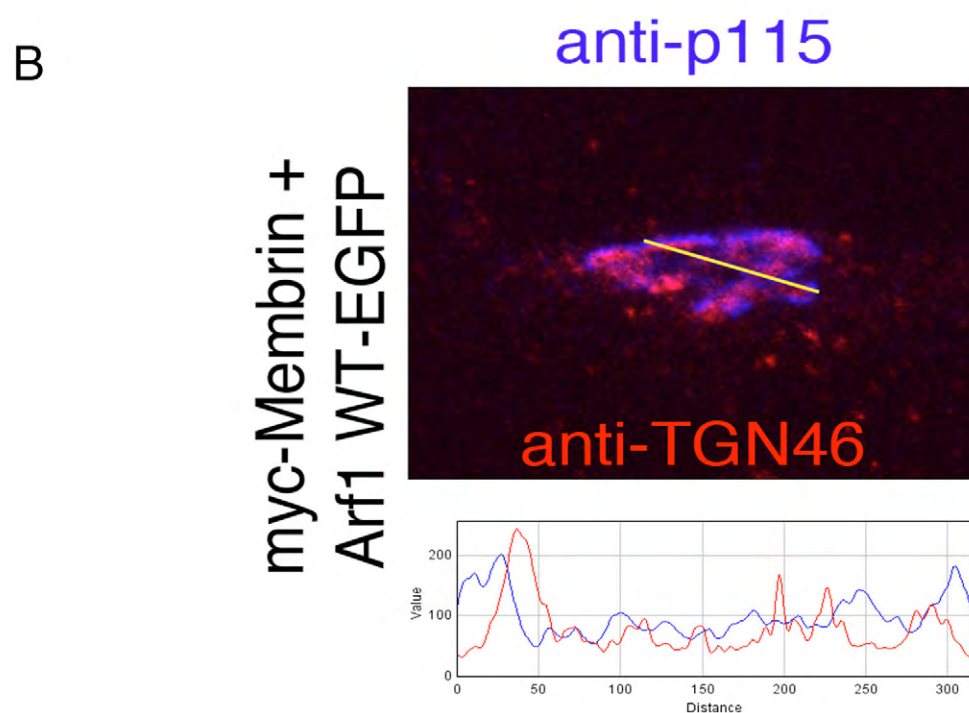
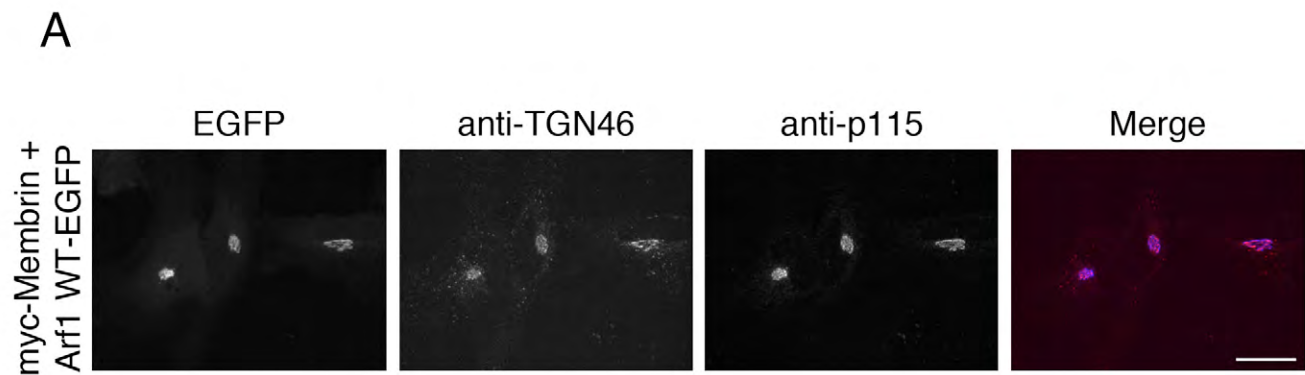
- De Matteis, M. A. and Luini, A. (2008). Exiting the Golgi complex. *Nat. Rev. Mol. Cell Biol.* **9**, 273–284.
- De Matteis, M. A., Di Campli, A. and Godi, A. (2005). The role of the phosphoinositides at the Golgi complex. *Biochim. Biophys. Acta* **1744**, 396–405.
- Dejgaard, S. Y., Murshid, A., Dee, K. M. and Presley, J. F. (2007). Confocal microscopy-based linescan methodologies for intra-Golgi localization of proteins. *J. Histochem. Cytochem.* **55**, 709–719.
- Doms, R. W., Russ, G. and Yewdell, J. W. (1989). Brefeldin A redistributes resident and itinerant Golgi proteins to the endoplasmic reticulum. *J. Cell Biol.* **109**, 61–72.
- Donaldson, J. G., Finazzi, D. and Klausner, R. D. (1992). Brefeldin A inhibits Golgi membrane-catalysed exchange of guanine nucleotide onto ARF protein. *Nature* **360**, 350–352.
- Donaldson, J. G., Honda, A. and Weigert, R. (2005). Multiple activities for Arf1 at the Golgi complex. *Biochim. Biophys. Acta* **1744**, 364–373.
- Dumaresq-Doiron, K., Savard, M. F., Akam, S., Costantino, S. and Lefrançois, S. (2010). The phosphatidylinositol 4-kinase PI4KIIIalpha is required for the recruitment of GBF1 to Golgi membranes. *J. Cell Sci.* **123**, 2273–2280.
- Emr, S., Glick, B. S., Linstedt, A. D., Lippincott-Schwartz, J., Luini, A., Malhotra, V., Marsh, B. J., Nakano, A., Pfeffer, S. R., Rabouille, C. et al. (2009). Journeys through the Golgi—taking stock in a new era. *J. Cell Biol.* **187**, 449–453.
- Farquhar, M. G. and Palade, G. E. (1998). The Golgi apparatus: 100 years of progress and controversy. *Trends Cell Biol.* **8**, 2–10.
- Franco, M., Chardin, P., Chabre, M. and Paris, S. (1993). Myristoylation is not required for GTP-dependent binding of ADP-ribosylation factor ARF1 to phospholipids. *J. Biol. Chem.* **268**, 24531–24534.
- Franco, M., Chardin, P., Chabre, M. and Paris, S. (1996). Myristoylation-facilitated binding of the G protein ARF1GDP to membrane phospholipids is required for its activation by a soluble nucleotide exchange factor. *J. Biol. Chem.* **271**, 1573–1578.
- Fujiwara, T., Oda, K., Yokota, S., Takatsuki, A. and Ikehara, Y. (1988). Brefeldin A causes disassembly of the Golgi complex and accumulation of secretory proteins in the endoplasmic reticulum. *J. Biol. Chem.* **263**, 18545–18552.
- Godi, A., Di Campli, A., Konstantakopoulos, A., Di Tullio, G., Alessi, D. R., Kular, G. S., Daniele, T., Marra, P., Lucocq, J. M. and De Matteis, M. A. (2004). FAPPs control Golgi-to-cell-surface membrane traffic by binding to ARF and PtdIns(4)P. *Nat. Cell Biol.* **6**, 393–404.
- Gommel, D. U., Memon, A. R., Heiss, A., Lottspeich, F., Pfannstiel, J., Lechner, J., Reinhard, C., Helms, J. B., Nickel, W. and Wieland, F. T. (2001). Recruitment to Golgi membranes of ADP-ribosylation factor 1 is mediated by the cytoplasmic domain of p23. *EMBO J.* **20**, 6751–6760.
- Haun, R. S., Tsai, S. C., Adamik, R., Moss, J. and Vaughan, M. (1993). Effect of myristoylation on GTP-dependent binding of ADP-ribosylation factor to Golgi. *J. Biol. Chem.* **268**, 7064–7068.
- Hay, J. C., Chao, D. S., Kuo, C. S. and Scheller, R. H. (1997). Protein interactions regulating vesicle transport between the endoplasmic reticulum and Golgi apparatus in mammalian cells. *Cell* **89**, 149–158.
- Helms, J. B. and Rothman, J. E. (1992). Inhibition by brefeldin A of a Golgi membrane enzyme that catalyses exchange of guanine nucleotide bound to ARF. *Nature* **360**, 352–354.
- Hofmann, I., Thompson, A., Sanderson, C. M. and Munro, S. (2007). The Arl4 family of small G proteins can recruit the cytohesin Arf6 exchange factors to the plasma membrane. *Curr. Biol.* **17**, 711–716.
- Honda, A., Al-Awar, O. S., Hay, J. C. and Donaldson, J. G. (2005). Targeting of Arf-1 to the early Golgi by membrin, an ER-Golgi SNARE. *J. Cell Biol.* **168**, 1039–1051.
- Ismail, S. A., Vetter, I. R., Sot, B. and Wittinghofer, A. (2010). The structure of an Arf-ARF-GAP complex reveals a Ca²⁺ regulatory mechanism. *Cell* **141**, 812–821.
- Kahn, R. A., Clark, J., Rulka, C., Stearns, T., Zhang, C. J., Randazzo, P. A., Terui, T. and Cavenagh, M. (1995). Mutational analysis of *Saccharomyces cerevisiae* ARF1. *J. Biol. Chem.* **270**, 143–150.
- Kawamoto, K., Yoshida, Y., Tamaki, H., Torii, S., Shinotsuka, C., Yamashina, S. and Nakayama, K. (2002). GBF1, a guanine nucleotide exchange factor for ADP-ribosylation factors, is localized to the cis-Golgi and involved in membrane association of the COPI coat. *Traffic* **3**, 483–495.
- Lippincott-Schwartz, J. (2011). An evolving paradigm for the secretory pathway? *Mol. Biol. Cell* **22**, 3929–3932.
- Lippincott-Schwartz, J., Yuan, L. C., Bonifacino, J. S. and Klausner, R. D. (1989). Rapid redistribution of Golgi proteins into the ER in cells treated with brefeldin A: evidence for membrane cycling from Golgi to ER. *Cell* **56**, 801–813.
- Liu, W., Duden, R., Phair, R. D. and Lippincott-Schwartz, J. (2005). ArfGAP1 dynamics and its role in COPI coat assembly on Golgi membranes of living cells. *J. Cell Biol.* **168**, 1053–1063.
- Lowery, J., Szul, T., Styers, M., Holloway, Z., Oorschot, V., Klumperman, J. and Sztul, E. (2013). The Sec7 guanine nucleotide exchange factor GBF1 regulates membrane recruitment of BIG1 and BIG2 guanine nucleotide exchange factors to the trans-Golgi network (TGN). *J. Biol. Chem.* **288**, 11532–11545.
- Manolea, F., Claude, A., Chun, J., Rosas, J. and Melançon, P. (2008). Distinct functions for Arf guanine nucleotide exchange factors at the Golgi complex: GBF1 and BIGs are required for assembly and maintenance of the Golgi stack and trans-Golgi network, respectively. *Mol. Biol. Cell* **19**, 523–535.
- Manolea, F., Chun, J., Chen, D. W., Clarke, I., Summerfeldt, N., Dacks, J. B. and Melançon, P. (2010). Arf3 is activated uniquely at the trans-Golgi network by brefeldin A-inhibited guanine nucleotide exchange factors. *Mol. Biol. Cell* **21**, 1836–1849.
- Mansour, S. J., Skaug, J., Zhao, X. H., Giordano, J., Scherer, S. W. and Melançon, P. (1999). p200 ARF-GEP1: a Golgi-localized guanine nucleotide exchange protein whose Sec7 domain is targeted by the drug brefeldin A. *Proc. Natl. Acad. Sci. USA* **96**, 7968–7973.
- Melançon, P., Zhao, X. and Lasell, T. K. (2003). Large Arf-GEFs of the Golgi complex: in search of mechanisms for the cellular effects of BFA. In *ARF Family GTPases* (ed. R. A. Kahn), pp. 101–119. Dordrecht: Kluwer Academic Publishers.
- Mossessova, E., Corpina, R. A. and Goldberg, J. (2003). Crystal structure of ARF1*Sec7 complexed with Brefeldin A and its implications for the guanine nucleotide exchange mechanism. *Mol. Cell* **12**, 1403–1411.
- Niu, T. K., Pfeifer, A. C., Lippincott-Schwartz, J. and Jackson, C. L. (2005). Dynamics of GBF1, a Brefeldin A-sensitive Arf1 exchange factor at the Golgi. *Mol. Biol. Cell* **16**, 1213–1222.
- Odorizzi, G., Babst, M. and Emr, S. D. (2000). Phosphoinositide signaling and the regulation of membrane trafficking in yeast. *Trends Biochem. Sci.* **25**, 229–235.
- Paris, S., Béraud-Dufour, S., Robineau, S., Bigay, J., Antonny, B., Chabre, M. and Chardin, P. (1997). Role of protein-phospholipid interactions in the activation of ARF1 by the guanine nucleotide exchange factor Arno. *J. Biol. Chem.* **272**, 22221–22226.
- Parnis, A., Rawet, M., Barkan, B., Rotman, M., Gaitner, M. and Cassel, D. (2006). Golgi localization determinants in ArfGAP1 and in new tissue-specific ArfGAP1 isoforms. *J. Biol. Chem.* **281**, 3785–3792.
- Pasqualato, S., Renault, L. and Cherfils, J. (2002). Arf, Arl, Arp and Sar proteins: a family of GTP-binding proteins with a structural device for ‘front-back’ communication. *EMBO Rep.* **3**, 1035–1041.
- Peyroche, A., Antonny, B., Robineau, S., Acker, J., Cherfils, J. and Jackson, C. L. (1999). Brefeldin A acts to stabilize an abortive ARF-GDP-Sec7 domain protein complex: involvement of specific residues of the Sec7 domain. *Mol. Cell* **3**, 275–285.
- Randazzo, P. A. and Kahn, R. A. (1995). Myristoylation and ADP-ribosylation factor function. *Methods Enzymol.* **250**, 394–405.
- Renault, L., Guibert, B. and Cherfils, J. (2003). Structural snapshots of the mechanism and inhibition of a guanine nucleotide exchange factor. *Nature* **426**, 525–530.
- Richardson, B. C. and Fromme, J. C. (2012). Autoregulation of Sec7 Arf-GEF activity and localization by positive feedback. *Small GTPases* **3**, 240–243.
- Richardson, B. C., McDonold, C. M. and Fromme, J. C. (2012). The Sec7 Arf-GEF is recruited to the trans-Golgi network by positive feedback. *Dev. Cell* **22**, 799–810.
- Robineau, S., Chabre, M. and Antonny, B. (2000). Binding site of brefeldin A at the interface between the small G protein ADP-ribosylation factor 1 (ARF1) and the nucleotide-exchange factor Sec7 domain. *Proc. Natl. Acad. Sci. USA* **97**, 9913–9918.
- Sáenz, J. B., Sun, W. J., Chang, J. W., Li, J., Bursulaya, B., Gray, N. S. and Haslam, D. B. (2009). Golgicide A reveals essential roles for GBF1 in Golgi assembly and function. *Nat. Chem. Biol.* **5**, 157–165.
- Sata, M., Donaldson, J. G., Moss, J. and Vaughan, M. (1998). Brefeldin A-inhibited guanine nucleotide-exchange activity of Sec7 domain from yeast Sec7 with yeast and mammalian ADP ribosylation factors. *Proc. Natl. Acad. Sci. USA* **95**, 4204–4208.
- Shiba, Y., Luo, R., Hinshaw, J. E., Szul, T., Hayashi, R., Sztul, E., Nagashima, K., Baxa, U. and Randazzo, P. A. (2011). ArfGAP1 promotes COPI vesicle formation by facilitating coatomer polymerization. *Cell. Logist.* **1**, 139–154.
- Shinotsuka, C., Waguri, S., Wakasugi, M., Uchiyama, Y. and Nakayama, K. (2002). Dominant-negative mutant of BIG2, an ARF-guanine nucleotide exchange factor, specifically affects membrane trafficking from the trans-Golgi network through inhibiting membrane association of AP-1 and GGA coat proteins. *Biochem. Biophys. Res. Commun.* **294**, 254–260.
- Szafer, E., Pick, E., Rotman, M., Zuck, S., Huber, I. and Cassel, D. (2000). Role of coatomer and phospholipids in GTPase-activating protein-dependent hydrolysis of GTP by ADP-ribosylation factor-1. *J. Biol. Chem.* **275**, 23615–23619.
- Szafer, E., Rotman, M. and Cassel, D. (2001). Regulation of GTP hydrolysis on ADP-ribosylation factor-1 at the Golgi membrane. *J. Biol. Chem.* **276**, 47834–47839.
- Szul, T., Garcia-Mata, R., Brandon, E., Shestopal, S., Alvarez, C. and Sztul, E. (2005). Dissection of membrane dynamics of the ARF-guanine nucleotide exchange factor GBF1. *Traffic* **6**, 374–385.
- Szul, T., Grabski, R., Lyons, S., Morohashi, Y., Shestopal, S., Lowe, M. and Sztul, E. (2007). Dissecting the role of the ARF guanine nucleotide exchange factor GBF1 in Golgi biogenesis and protein trafficking. *J. Cell Sci.* **120**, 3929–3940.
- Tsai, S. C., Adamik, R., Moss, J. and Vaughan, M. (1996). Purification and characterization of a guanine nucleotide-exchange protein for ADP-ribosylation factor from spleen cytosol. *Proc. Natl. Acad. Sci. USA* **93**, 305–309.
- Zhao, X., Lasell, T. K. and Melançon, P. (2002). Localization of large ADP-ribosylation factor-guanine nucleotide exchange factors to different Golgi compartments: evidence for distinct functions in protein traffic. *Mol. Biol. Cell* **13**, 119–133.
- Zhao, X., Claude, A., Chun, J., Shields, D. J., Presley, J. F. and Melançon, P. (2006). GBF1, a cis-Golgi and VTCs-localized ARF-GEF, is implicated in ER-to-Golgi protein traffic. *J. Cell Sci.* **119**, 3743–3753.



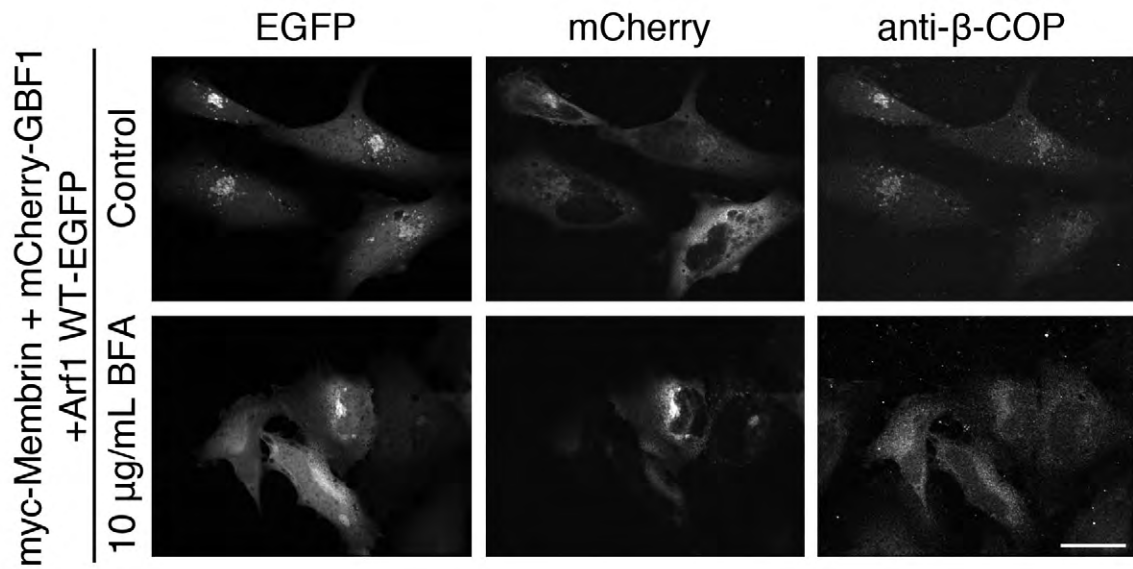
Supplementary Figure 1 Western blot analysis of extracts from cells expressing Arf1-EGFP. (A and B) Uncropped western blots show low level over-expression of Arf1-EGFP constructs. Western blot analysis of post-nuclear extracts prepared from HeLa cells transfected as described in legend to Figure 2A. Membranes were incubated with mouse anti-Arf 1D9 (A) and rabbit anti-GFP (B) and were developed and analyzed. Image shown corresponds to uncropped blot from which panels shown in Figure 2A were obtained. (C) Expression of tagged Arfs does not alter the level of endogenous GBF1. Western blot analysis of post-nuclear extracts prepared from HeLa cells transfected as described in legend to Figure 2A. Membrane was incubated with mouse anti-GBF1 and was then developed and analyzed.



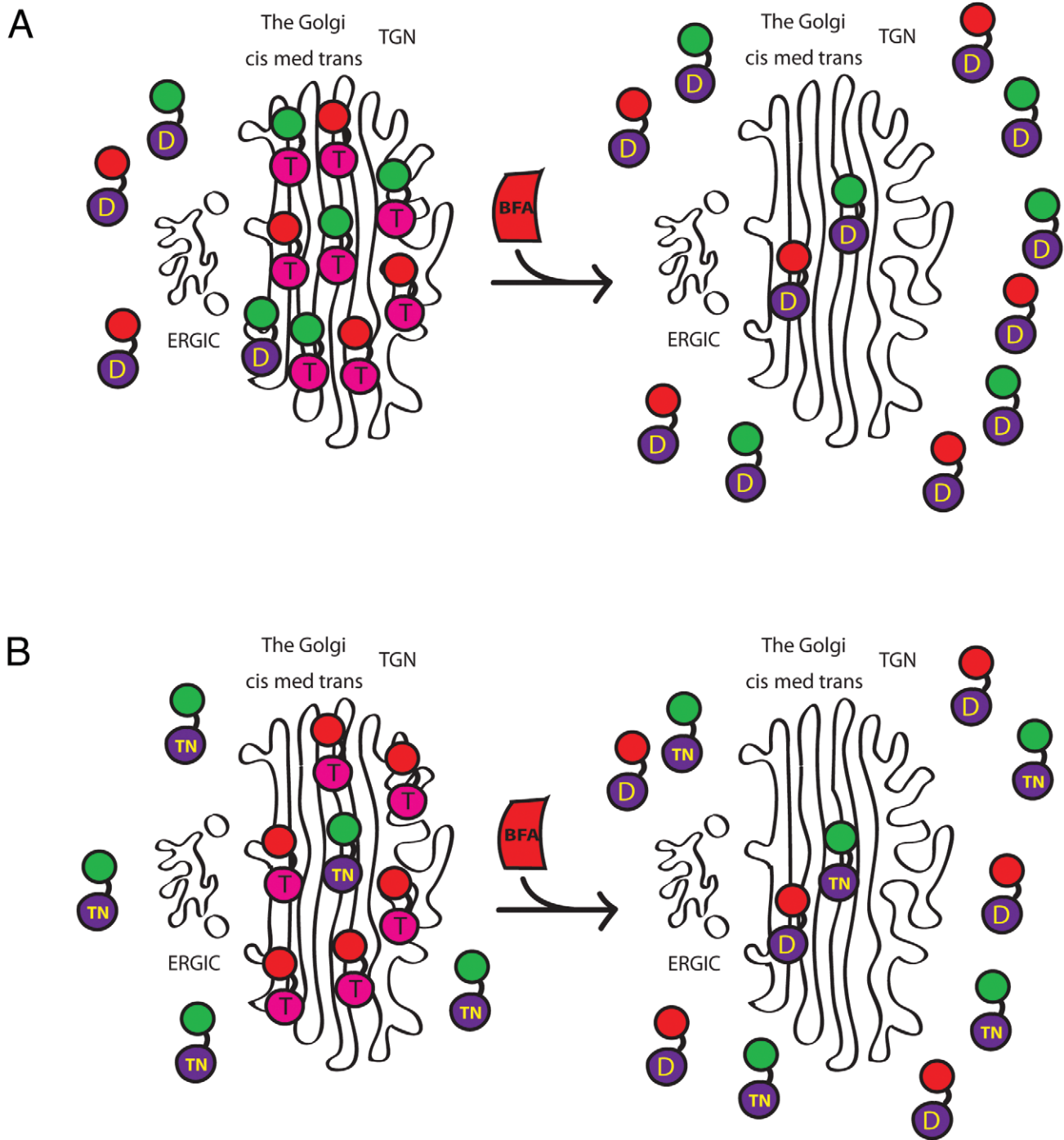
Supplementary Figure 2 Exogenous expression of myc-membrin is not required for Arf1 T31N-dependent GBF1 accumulation on Golgi membranes. HeLa cells were co-transfected with plasmids encoding mCherry-GBF1 with or without myc-membrin, and either Arf1 WT-EGFP or Arf1 T31N-EGFP. Cells were then fixed and stained with mouse anti-membrin monoclonal antibody and imaged as for Response Figure 1 (n=3). Scale bars = 26 μ m. These images indicate that the presence or absence of exogenously expressed myc-membrin has no effect on GBF1 localization and does not alter the recruitment phenotype observed with the expression of TN mutant Arf1. Further, it does not appear that myc-membrin expression increases the amount of Arf1 TN-EGFP associated with Golgi membranes, as one may expect if membrin is a strong binder of Arf1•GTP. Images obtained of endogenous membrin staining required at least 20x longer exposure time compared to those expressing exogenous myc-membrin, suggesting significant over-expression of the myc-membrin.



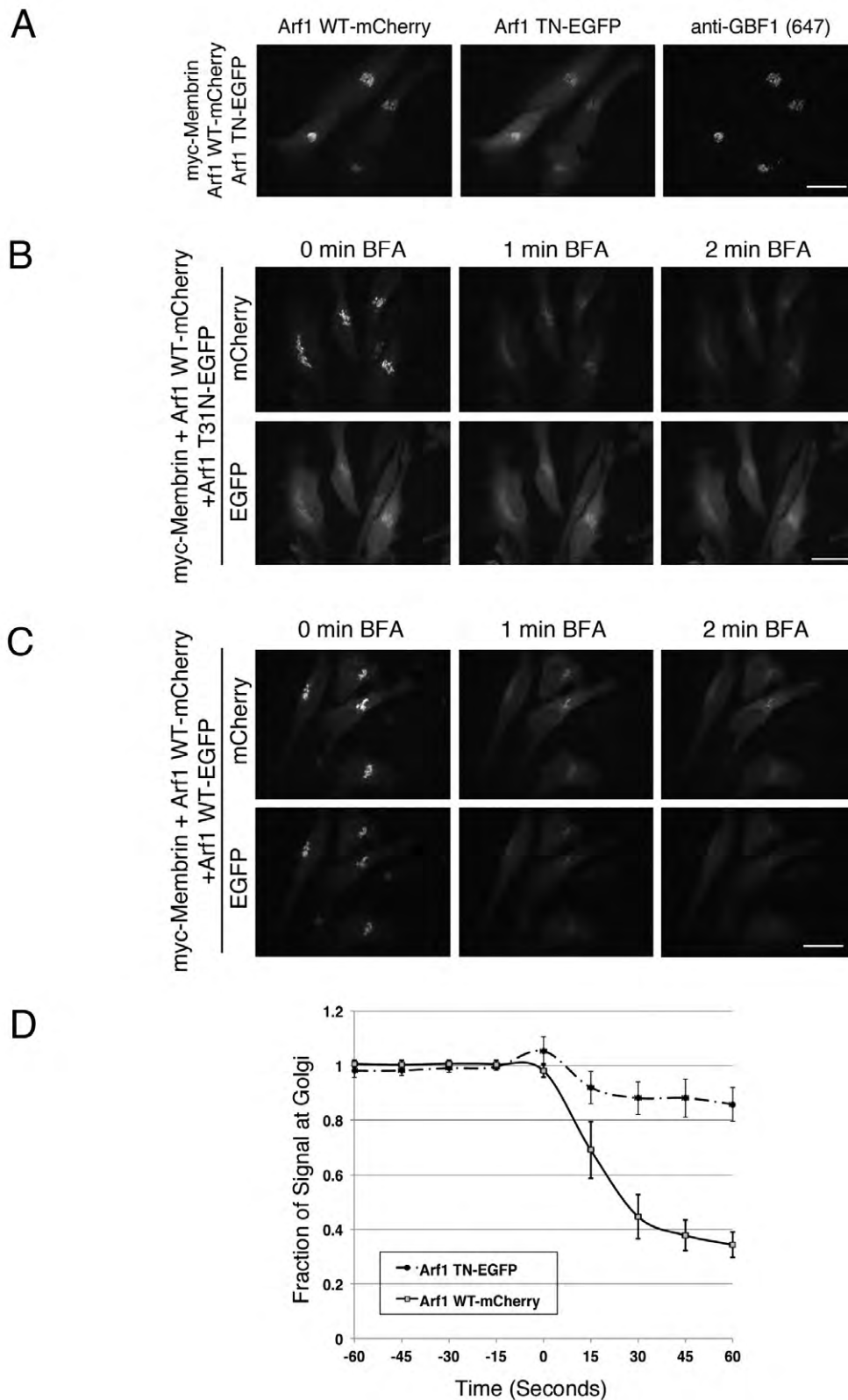
Supplementary Figure 3 Golgi polarization revealed by p115 and TGN46 separation in cell expressing Arf1 WT-EGFP. (A) HeLa cells were co-transfected with plasmids encoding myc-membrin and Arf1 WT-EGFP, fixed and stained with sheep anti-TGN46 and mouse anti-p115 and then imaged as for Figure 1 (n=3). (B) Line scan analysis was performed on cells expressing myc-membrin and Arf1 WT-EGFP and stained with sheep anti-TGN46 and mouse anti-p115. A 4-fold magnification of a representative Golgi from A is shown.



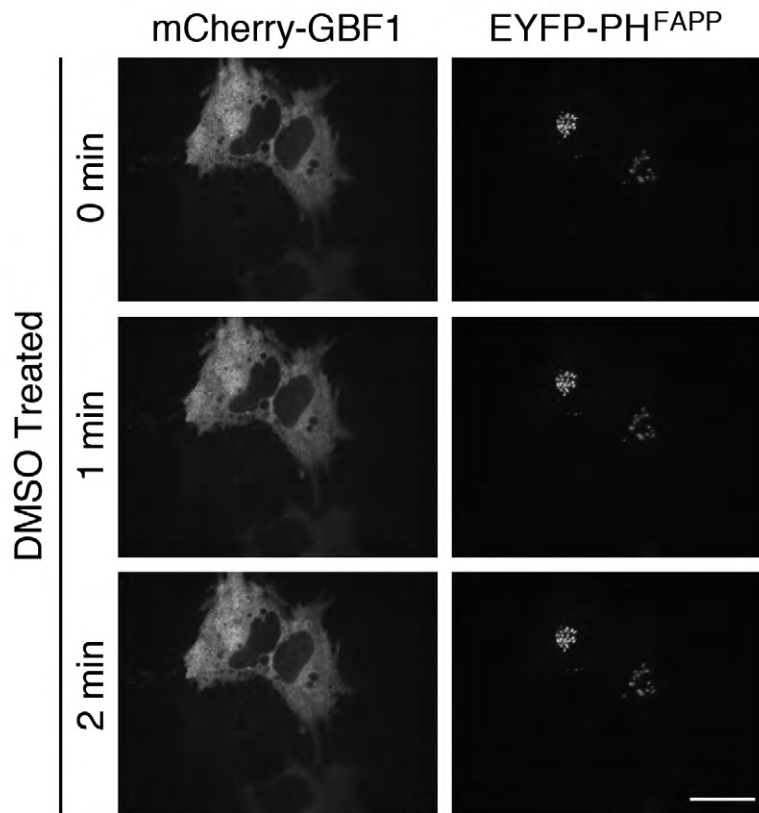
Supplementary Figure 4 COPI localization to Golgi membranes is GBF1-dependent in cells expressing Arf1 WT-EGFP. (A) HeLa cells co-transfected with plasmids encoding myc-membrin and Arf1 WT-EGFP were treated with either 10 μ g/mL BFA or DMSO control for 20 min. They were then fixed, stained with mouse anti- β -COP, and imaged as for Figure 1.



Supplementary Figure 5 Diagram illustrating expected experimental outcomes with cells expressing both mCherry and GFP-tagged Arfs. (A) Cells expressing both WT Arf1-GFP and WT Arf1-mCherry are depicted before (left) and after (right) treatment with BFA. Before BFA treatment the majority of tagged Arfs accumulate in the GTP-bound form on Golgi membranes. BFA treatment causes conversion of tagged-Arfs to the GDP-bound form that redistributes predominantly to cytosol. **(B)** Cells expressing both WT Arf1-mCherry and T31N Arf1-GFP are depicted before (left) and after (right) treatment with BFA. Before BFA treatment the majority of mCherry-tagged WT Arfs accumulate in the GTP-bound form on Golgi membranes while mutant GFP-tagged Arf is predominantly cytosolic. BFA treatment causes conversion of mCherry-tagged WT Arf to the GDP-bound form that redistributes predominantly to cytosol. In all cases, some tagged-Arfs remain Golgi-localized in a GDP-bound form.



Supplementary Figure 6 GBF1 remains catalytically active following Arf•GDP-dependent recruitment. (A) HeLa cells were co-transfected with plasmids encoding myc-membrin and both WT Arf1-mCherry and T31N Arf1-EGFP. Cells were then fixed and stained with mouse anti-GBF1 monoclonal antibody and imaged as for Figure 1 (n=3). (B) Live HeLa cells expressing Arf1 T31N-EGFP and Arf1 WT-mCherry were treated with 5 μ g/mL BFA and imaged as for Figure 1. (C) Live HeLa cells expressing Arf1 WT-mCherry and Arf1 WT-EGFP were treated with 5 μ g/mL BFA and imaged as for Figure 1. (D) Quantification of the normalized fraction of Arf signal at the Golgi was performed on cells expressing Arf1 WT-mCherry and either Arf1 WT-EGFP or Arf1 T31N-EGFP treated with 5 μ g/mL BFA. A minimum of 2 cells similar to those shown in panel B were quantitated in each of 4 separate experiments. Images from panels B and C obtained before BFA addition were used to assemble Fig. 4B.



Supplementary Figure 7 Arf•GDP-dependent GBF1 recruitment to *cis*-Golgi membranes is independent of PI4P levels. HeLa cells expressing mCherry-GBF1 and EYFP-PH^{FAPP} were treated with carrier DMSO at the same final concentration as in Figure 5 and imaged by live cell spinning disc confocal microscopy as for Figure 1 (n=6). Scale bars = 26 μ m.